INVESTIGATION OF SITE-SPECIFIC METAL-CATALYZED OXIDATION OF PROTEINS USING DIPEPTIDES AS MODEL COMPOUNDS

by

Kathleen A. Kwolek

Submitted in Partial Fulfillment of the Requirements
for the Degree of
Master of Science
in the
Chemistry
Program

YOUNGSTOWN STATE UNIVERSITY

August, 1998

INVESTIGATION OF SITE-SPECIFIC

METAL-CATALYZED OXIDATION OF PROTEINS

USING DIPEPTIDES AS MODEL COMPOUNDS

Kathleen A. Kwolek

I hereby release this thesis to the public. I understand this thesis will be housed at the Circulation Desk of the University library and will be available for public access. I also authorize the University or other individuals to make copies of this thesis as needed for scholarly research.

Signature: Kathleen A. Kwolek 8-18-98

Kathleen A. Kwolek — Date

Approvals: Michael A. Serra 8/18/98

Dr. Michael Serra — Date
Thesis Advisor

Renee Falconer 8/11/98

Dr. Renee Falconer — Date
Committee Member

James H Mike 8/14/98

Dr. James Mike — Date
Committee Member

Peter J Kasvinsky 8/19/98

Dr. Peter J. Kasvinsky — Date
Dean of Graduate Studies

ABSTRACT

INVESTIGATION OF SITE-SPECIFIC METAL-CATALYZED OXIDATION OF PROTEINS USING DIPEPTIDES AS MODEL COMPOUNDS

Kathleen A. Kwolek

Youngstown State University

Although oxidative damage to proteins has been a subject of intense investigation, very little has been elucidated regarding the site-specificity of this damage due to reactive oxygen species. The extremely reactive hydroxyl radical should cause damage to the polypeptide in the vicinity of its reaction with metal ions bound to the chain. This paper investigates the site-specificity of metal-catalyzed oxidation of dipeptides using metal ions and hydrogen peroxide to generate the hydroxyl radical. A variety of conditions (different dipeptides, metal ions, temperatures and pH) were explored. Ultraviolet spectroscopy and thin layer chromatography were used to monitor reactions. Purification of reaction products was attempted through lyophilization. Endeavors to separate the mixture after reaction used percolation column chromatography and high performance liquid chromatography.

ACKNOWLEDGMENTS

I would like to thank Dr. Michael Serra for his guidance and insight, both in my research and in the writing of this thesis. I would also like to thank Dr. J. Yemma for the use of his lyophilization equipment, Dr. James Mike for his patience and help with the function of the HPLC, and to Dr. Renee Falconer for her encouragement to see this project to completion.

TABLE OF CONTENTS

LIST OF ABBREVIATIONS

BHT	butylated hydroxytoluene
CBZ-GX	carbobenzoxyamino acid
DNA	deoxyribonucleic acid
EDTA	ethylene diamine tetraacetic acid
ε_m	extinction coefficient
e.s.r.	electron spin resonance
GLDH	L-glutamate dehydrogenase
GSH	glutathione
GSHPX	glutathione peroxidases
GXC	dipeptide control
GXFe	dipeptide with iron ion
GX(h)	dipeptide with hydroxyl radical incubated for "h" hours
GXP	dipeptide with hydrogen peroxide
HAc	acetic acid
HFBA	heptafluorobutyric acid
$HO_2^{\bullet}$	hydroperoxy radical
HPLC	high performance liquid chromatography
k	rate constant
KPi	potassium phosphate buffer
LOOH	lipid peroxides
MCO	metal-catalyzed oxidation
min	minutes

$M^{-1}sec^{-1}$	per molar per second	
NaAc	sodium acetate	
NADH	nicotinamide adenine dinucleotide	
NADPH	nicotinamide adenine dinucleotide phosphate	
NMR	nuclear magnetic resonance	
$NO^{\bullet}$	nitric oxide	
$NO_2^{\bullet}$	nitric dioxide	
$O_2^{\bullet}$	superoxide radical	
$^1O_2$	singlet oxygen	
O_2^{2-}	peroxide ion	
$OH^{\bullet}$	hydroxyl radical	
$ONOO^-$	peroxynitrate	
psi	pounds per square inch	
R_f	retention factor	
ROS	reactive oxygen species	
RP	reversed-phase	
SOD	superoxide dismutase	
TLC	thin layer chromatography	
A	Ala	alanine
C	Cys	cysteine
E	Glu	glutamic acid
G	Gly	glycine
H	His	histidine
M	Met	methionine
P	Pro	proline

Y	Tyr	tyrosine
AGY	acetylated Gly-Tyr	acetylated glycyltyrosine
AY	Ala-Tyr	alanyltyrosine
GE	Gly-Glu	glycylglutamine
GF	Gly-Phe	glycylphenylalanine
GG	Gly-Gly	glycylglycine
GH	Gly-His	glycylhistidine
GM	Gly-Met	glycylmethionine
GP	Gly-Pro	glycylproline
GS	Gly-Ser	gylcylserine
GW	Gly-Trp	glycyltryptophan
GY	Gly-Tyr	glycyltyrosine
PY	Pro-Tyr	prolyltyrosine
YG	Tyr-Gly	tyrosylglycine

LIST OF FIGURES

LIST OF SCHEMES

LIST OF TABLES

CHAPTER 1

INTRODUCTION AND HISTORICAL BACKGROUND

Free radical chemistry has become an intensive research topic in recent years (*1*). Reactive oxygen species (ROS) including the superoxide radical ($O_2^{\bullet}$), hydrogen peroxide (H_2O_2), the hydroxyl radical ($OH^{\bullet}$) and lipid peroxides (LOOH) are believed to be responsible for oxidative damage to a broad array of biomolecules (*1*). The modification of nucleic acids, lipids and proteins by oxygen free radicals suggests they play a role in the pathogenesis of several diseases (*1*). For example, free radical damage and the accumulation of subsequently deactivated biomolecules is an apparent manifestation of several disease states, including muscular dystrophy, rheumatoid arthritis, pulmonary emphysema as well as the process of aging.

Random oxidation of the side chains of many different amino acids, extensive fragmentation of protein chains, cleavage of peptide bonds, and the production of cross-linked derivatives of proteins are typically observed in studies of the interactions between ROS produced by ionizing radiation and amino acids, peptides and proteins (*2*). In direct contrast, when proteins are exposed to metal-catalyzed oxidation (MCO) systems consisting of O_2 or H_2O_2 and transition metals, only a few amino acid residues are modified and little peptide bond fragmentation occurs (*2*). MCO systems catalyze the production of ROS via the interaction of transition metal ions and H_2O_2, followed by attack on nearby amino acid side chains.

In the following sections, the nature of ROS and their reactions on proteins with respect to both environmental and physiological exposures is examined. The roles of antioxidant defense mechanisms in the body and the consequences of oxidative stress will be discussed, followed by an exploration of the processes of metal-catalyzed oxidation (MCO) of proteins.

A great deal of what we presently know about ROS was first learned by studying the damage produced by ionizing radiation, which also produces ROS. Thus, a detailed look at protein modification via ionizing radiation is presented.

Reactive Oxygen Species

Any species with one or more unpaired electrons in an orbital is considered to be a free radical. Examples include the hydrogen atom, the oxygen molecule, most transition elements, $NO^{\bullet}$ (nitric oxide), and $NO_2^{\bullet}$ (nitric dioxide). When a radical reacts with a non-radical species, new radicals are produced. Only when two radicals join their unpaired electrons will the reaction terminate.

Ground state diatomic oxygen contains two unpaired electrons with parallel spin in separate π^* antibonding orbitals (Figure 1a). Although a free radical, diatomic oxygen has relatively low reactivity with biological molecules. Since oxygen can only accept two electrons with parallel spins, its valence shell is spin-restricted with respect to biomolecules, which have paired electrons with opposite spins. Thus oxygen accepts its electrons one at a time, slowing reactions with non-radical species. Alleviation of this spin restriction can occur by moving one of the unpaired electrons. Excitation of oxygen by illumination can create singlet oxygen ($^1O_2$), in which one of the unpaired electrons moves to share the π^* antibonding orbital of the other electron (Figure 1b). Singlet oxygen is no longer a radical. The superoxide radical ($O_2^{\bullet}$) results when a diatomic oxygen molecule gains one electron in a half-filled π^* antibonding orbital (Figure 1c) (*3*).

(a) Ground State $\sigma 1s^2\ \sigma^*1s^2\ \sigma 2s^2\ \sigma^*2s^2\ \sigma 2p^2\ \pi 2p_x^2\ \pi 2p_y^2\ \pi^*2p_x^1\ \pi^*2p_y^1$

(b) Singlet $^1O_2$ $\sigma 1s^2\ \sigma^*1s^2\ \sigma 2s^2\ \sigma^*2s^2\ \sigma 2p^2\ \pi 2p_x^2\ \pi 2p_y^2\ \pi^*2p_x^2$

(c) Superoxide $\sigma 1s^2\ \sigma^*1s^2\ \sigma 2s^2\ \sigma^*2s^2\ \sigma 2p^2\ \pi 2p_x^2\ \pi 2p_y^2\ \pi^*2p_x^2\ \pi^*2p_y^1$

(d) Peroxide $\sigma 1s^2\ \sigma^*1s^2\ \sigma 2s^2\ \sigma^*2s^2\ \sigma 2p^2\ \pi 2p_x^2\ \pi 2p_y^2\ \pi^*2p_x^2\ \pi^*2p_y^2$

Figure 1 Electron Configuration of Various Diatomic Oxygen Species (*3*)

If the superoxide ion becomes protonated, which can occur near activated macrophages with pH ~ 5, the $HO_2^\bullet$ (hydroperoxy) radical is generated (eq 1). This species may cross through membranes, possibly reacting with fatty acids to produce peroxides. $O_2^\bullet$ can undergo a dismutation reaction in aqueous solution (eq 2), producing H_2O_2. With no unpaired electrons, H_2O_2 is limited in direct activity but can easily pass through cell membranes. At high levels, H_2O_2 can inactivate the glycolytic enzyme glyceraldehyde-3-phosphate dehydrogenase (*4*). If an additional electron is gained by $O_2^\bullet$, the peroxide ion (O_2^{2-}) is produced (Fig 1d). At physiological pH, peroxide is protonated to produce hydrogen peroxide (H_2O_2) (eq. 3)

$$O_2^\bullet + H^+ \longrightarrow HO_2^\bullet \quad (1)$$

$$2O_2^\bullet + 2\,H^+ \longrightarrow H_2O_2 + O_2 \quad (2)$$

$$O_2^{2-} + 2\,H^+ \longrightarrow H_2O_2 \quad (3)$$

The generation of ROS can occur through a variety of different processes, including both environmental mechanisms and metabolic pathways (*5*). X-rays or γ - rays can produce hydroxyl radicals via the homolytic fission of O-H bonds in H_2O. Formation of singlet oxygen occurs upon an organism's exposure to UV rays, and ozone or NO_2 in

the atmosphere react to create a variety of NO radicals. The most relevant of these species to biological molecules is singlet oxygen. Systems containing pigments can absorb light, enter a higher electronic energy state, where they are able to transfer the energy to oxygen resulting in the singlet state. One example of a pigmented system is the lens of the eye (*6*). Excessive formation of singlet oxygen occurs in patients with porphyria, in which errors in porphyrin metabolism cause extreme light sensitivity (*7*).

Several metabolic processes also result in the production of ROS. Endogenous oxidases produce H_2O_2 which is used by thyroid peroxidase to make hormones. Glutathione peroxidases (GSHPX) use H_2O_2 to oxidize glutathione (GSH) (*4*). Lipid peroxidation produces alkyl radicals, alkylperoxy radicals and alkyl peroxides. Nitric oxide synthase acts on arginine to produce the nitric oxide radical. The superoxide radical (the one-electron reduced form of O_2) is generated by the loss of electrons onto O_2 from the electron transport chain of cells and during the respiratory burst of phagocytic cells (*6*). These radicals aid in the destruction of bacteria and regulation of acute inflammation (*3*). Neutrophils and macrophages produce $O_2^{\bullet}$ and H_2O_2. During the transfer of electrons in the terminal respiratory chain, auto-oxidation of electron carriers like $FADH_2$ can produce H_2O_2 and $O_2^{\bullet}$ (*6*). Superoxide can also attack iron-sulfur clusters at the active site of an enzyme (*3*). Although $O_2^{\bullet}$ is fairly unreactive in aqueous solutions, the interior of biological membranes is hydrophobic and systems that produce this radical show evidence of biological damage. $O_2^{\bullet}$ can react with $NO^{\bullet}$, producing peroxynitrate ($ONOO^-$). As $NO^{\bullet}$ regulates smooth muscle tone to control blood pressure, vasoconstriction occurs with loss of $NO^{\bullet}$. $O_2^{\bullet}$ may also destroy phospholipids by nucleophilic attack (*4*), and the ester bonds linking fatty acids to glycerol may be vulnerable to $O_2^{\bullet}$ damage at their carbonyl groups (*3*).

Transition metals are capable of accepting and donating one electron at a time, and can increase the reactivity of oxygen by overcoming its spin-restriction. Such metals are

often found at the active sites of biomolecules involved with oxygen-derived species. Upon contact with various metal ions such as Ti(III), Cu(I), Fe(II), and Co(II), H_2O_2 can generate the even more reactive hydroxyl radical ($OH^{\bullet}$). The Fenton Reaction uses Fe(II) and H_2O_2, initially producing the hydroxyl radical and the hydroxide ion (eq 4). Newly formed Fe(III) can further react with H_2O_2, generating superoxide (eq 5).

$$Fe^{2+} + H_2O_2 \longrightarrow Fe^{3+} + OH^{\bullet} + OH^{-} \quad (4)$$

$$Fe^{3+} + H_2O_2 \longrightarrow Fe^{2+} + O_2^{\bullet} + 2\,H^{+} \quad (5)$$

Other possible reactions include (*3*):

$$OH^{\bullet} + H_2O_2 \longrightarrow H_2O + H^{+} + O_2^{\bullet} \quad (6)$$

$$OH^{\bullet} + Fe^{2+} \longrightarrow Fe^{3+} + OH^{-} \quad (7)$$

Cu(I) reacts with H_2O_2 in a similar manner but with a much higher rate constant that Fe(II) (*3*).

The hydroxyl radical is the most reactive of ROS, reacting with all classes of biomolecules with extremely high rate constants ($k = 10^9\text{-}10^{10}\ M^{-1}sec^{-1}$) (*3*). Reactions are of three types: abstraction of a hydrogen atom (eq 8), addition (e.g. with the aromatic rings of DNA), and electron transfer (eq 9) (*3*).

$$CH_3OH + OH^{\bullet} \longrightarrow H_2O + {}^{\bullet}CH_2OH \quad (8)$$

$$Cl^{-} + OH^{\bullet} \longrightarrow Cl^{\bullet} + OH^{-} \quad (9)$$

Such activity would make it likely for $OH^{\bullet}$ to react in the vicinity near its site of production, producing a new, less reactive radical. Such secondary radicals are able to

move further from their initial site of formation to attack other biological species. The $OH^{\bullet}$ radical is found to be formed in various $O_2^{\bullet}$ generating systems, such as activated phagocytes and hypoxanthine/xanthine oxidase mixtures. $O_2^{\bullet}$ is thought to react with H_2O_2 as shown in equation (10):

$$H_2O_2 + O_2^{\bullet} \longrightarrow O_2 + OH^- + OH^{\bullet} \qquad (10)$$

Formation of $OH^{\bullet}$ through this mechanism has been detected by its ability to affect hydroxylation of aromatic compounds, attacks on tryptophan, and production of an e.s.r. signal (*3*). However, the rate constant for these reactions is nearly zero in aqueous solution without traces of transition metals. Thus, a possible mechanism involves the reduction of Fe(III) to Fe(II) by $O_2^{\bullet}$ (eq 11), followed by reaction of Fe(II) with H_2O_2 (the Fenton reaction, eq 4).

$$O_2^{\bullet} + Fe^{3+} \longrightarrow Fe^{2+} + O_2 \qquad (11)$$

Antioxidant Defense Mechanisms

Due to the highly reactive nature of the $OH^{\bullet}$ and its damaging effects on biomolecules, a number of antioxidant defense mechanisms have been developed to prevent the production of ROS. These cellular defense mechanisms take a variety of forms including the sequestering of transition metals, the conversion of ROS to less reactive species and the use of a variety of antioxidants which terminate free radical chain reactions.

Iron ions are sequestered *in vivo* by being bound to the transport protein transferrin, and the storage proteins ferritin and hemosiderin. Dietary iron exists as Fe(III) until reduced by vitamin C in the stomach to Fe(II), which then enters the transferrin

protein via the gut. Transferrin has two separate binding sites for the iron. Although approximately 30% of the transferrin is loaded with iron, the tight binding permits essentially no free iron ion in blood plasma. The transferrin delivers the iron into various cells for use by enzymes and proteins requiring iron as a co-factor. Any additional iron not used by these compounds is stored in ferritin (4500 moles of iron per mole of ferritin). The iron enters ferritin as Fe(II), becoming oxidized and deposited as Fe(III). The ferritin molecule is surrounded by a shell (apoferritin), preventing excess free iron from accumulating within the cell. In order for removal to occur, the Fe(III) must be reduced by agents such as cysteine. The small amount of non-protein bound iron could provide the source of iron for the Fenton reaction (*3*).

Although the body contains approximately 80 mg copper, most of it is tightly bound to serum albumin. In the liver, the copper is attached to the glycoprotein ceruloplasmin, which only releases the copper when degraded.

In vitro, the production of $OH^{\bullet}$ radicals from the Cu(I) ion and H_2O_2 is prevented by adding physiological concentrations of histidine or albumin. However, albumin does not prevent Fe(II) from forming $OH^{\bullet}$. When using Cu(II) bound to histidine or albumin, $O_2^{\bullet}$ is able to reduce Cu(II), making it likely to produce $OH^{\bullet}$ (*3*).

Being less reactive than $OH^{\bullet}$, $O_2^{\bullet}$ and H_2O_2 may diffuse some distance from their origin once formed (*3*). H_2O_2 can cross cell membranes while $O_2^{\bullet}$ cannot. DNA damage or the initiation of lipid peroxidation by membrane lipids can result if either species have bound metal ions. Should a protein-bound metal ion react with $O_2^{\bullet}$ or H_2O_2, $OH^{\bullet}$ is likely formed at that site. Other reducing agents, such as NADH, NADPH, and thiol compounds have also been found to interact with metal ions and H_2O_2 to produce $OH^{\bullet}$ radicals (*3*).

Superoxide dismutase (SOD) enzymes are specific antioxidants which remove $O_2^{\bullet}$ from cells by converting it to H_2O_2 (eq 12). Mn-SOD is found in human mitochondria,

and Cu,Zn-SOD is found in the cytosol. The catalyst has a surface charge arrangement which uses $O_2^{\bullet}$ as a substrate.

$$2\,O_2^{\bullet} + 2\,H^{+} \longrightarrow H_2O_2 + O_2 \qquad (12)$$

Ischemia/reperfusion injury is prevented by SOD. These enzymes are present in all aerobic organisms and thought to be a first line of defense against specific ROS (*7*). Inhibition of $OH^{\bullet}$ producing reactions (eq. 4,10) can occur with SOD and a second antioxidant enzyme, catalase. Catalase contains a heme group in each of its 4 subunits and uses H_2O_2 as both an electron donor and an electron acceptor (eq 13).

$$H_2O_2 + H_2O_2 \longrightarrow 2\,H_2O + O_2 \qquad (13)$$

In addition, mannitol, formate and thiourea act as free radical scavengers and protect against damage caused by $O_2^{\bullet}$ generating systems (*3*).

In the extracellular environment, SOD, GSH, GSHPX and catalase levels are low; transition metal ions are sequestered to prevent catalysis of free radical reactions. Inside cell membranes, α-tocopherol is an important free-radical scavenger since oxidation of the membrane by ROS causes a free-radical chain reaction (lipid peroxidation) to occur.

Oxidative Stress

Antioxidants protect against unproductive free radicals and defense systems exist to repair damage. In general, there is a balance between the generation of ROS and antioxidant defense activity. Oxidative stress occurs when defense mechanisms are overwhelmed, resulting in oxidative damage to proteins, lipids and DNA. Oxidative stress results in tissue injury, which may release stored metal ions. Levels of free iron increase when proteins normally binding these ions are damaged (*4*). Inflammatory sites exposed

to acidic environments can generate free iron (*7*). The released iron ion can lead to $OH^{\bullet}$ production. Excess production of ROS at sites of chronic inflammation can cause severe damage, as in the inflamed joints of rheumatoid arthritis patients and in the stomachs of those with inflammatory bowel disease (*4*). Irregularities in the metabolism of iron occurs with rheumatoid arthritis; iron proteins are deposited in synovial membranes as hemoglobin concentration falls. Many inflammatory conditions, infections and tissue injury are accompanied by a loss of total iron in the blood (*3*). Malignancies produce changes in the body's iron distribution, with iron in the blood relocating to the liver, spleen and bone marrow (*3*).

Oxidative stress leads to increased levels of protein carbonyls. The following examples show elevated amounts of carbonyls when experiencing a variety of stressors: the lung tissue of rats exposed to hypoxia (*8*), the hind leg muscle of rats subjected to exercise (*9*), the brain of gerbils reacting to ischemia-reperfusion (*10*), human plasma exposed to ozone (*11*) or cigarette smoke (*12*), the heart and brain of mice exposed to X-rays (*13*), and the liver of mice in response to alcohol (*14*).

The level of oxidized protein in the tissue of subjects with certain diseases is higher than in healthy subjects (*15*). Levels of protein carbonyl groups in the synovial fluid of rheumatoid arthritic patients is elevated. It is believed the MCO of low density lipoproteins is subsequently taken up by macrophages to form foam cells which may develop into atherosclerosis. It has been found that free radicals are generated during ischemia/reperfusion, causing tissue damage. In neurological disorders, myelin proteins generate carbonyl groups when incubated with MCO systems, followed by rapid degradation by myelin proteases. In cataractogenesis, there is a small increase in the protein carbonyl content of the human lens with aging (*16*). Evidence indicates that the accumulation of inactive forms of many enzymes is age-related. Measurement of the concentration of protein carbonyl groups has been proposed as a test for the involvement

of MCO reactions in the aging process (*16*). Over 10-80 years of age, there is an exponential increase in the level of protein carbonyl groups. Individuals with premature aging diseases, such as progeria or Werner's syndrome, had protein carbonyl levels similar to those found in normal 80-year-olds (*16*). In addition, the level of active proteases responsible for the degradation of oxidized protein also decreases with age. In young animals, the amount of oxidized protein is approximately 10% of the total protein; whereas, this amount approaches 30% in older animals.

Metal-Catalyzed Oxidation

The main source of hydroxyl radical *in vivo* is the metal-catalyzed cleavage of hydrogen peroxide (*5*). The location of the metal ion catalysts required for $OH^{\bullet}$ generation is a major factor determining the site of possible damage. With high concentrations of Fe(II) and H_2O_2 (not found under normal physiological conditions), all amino acids are targets of attack, resulting in peptide bond cleavage and cross-linking of proteins (*17*). With low concentrations (as found in the body), protein modification occurs only at the metal binding sites of the protein. Hydroxyl scavengers do not inhibit this modification. Thus, it is proposed that metal-catalyzed modification of proteins at physiological conditions is a site-specific process where the transition metal and H_2O_2 react at the metal-binding site to generate hydroxyl radicals, which in turn attack the side chains of nearby amino acid residues and the peptide bond (*18,19*). For some enzymes, this is followed by conversions of amino acids to carbonyl derivatives, a decrease in catalytic activity, and to protein degradation. Catalase prevents these modifications; therefore, inhibition of the enzyme's modification in its presence indicates hydrogen peroxide's role in these processes. Evidence of site-specificity includes the fact that only a few amino acids on the protein are modified and most modified proteins contain metal-binding sites (*16*). Studies show that MCO systems may be partially responsible for

the alteration of proteins *in vivo* as well as the amassing of altered enzymes during aging (*2*). It has been proposed that metal-catalyzed oxidation of proteins marks them for degradation (*6*). As an example, glutamine synthetase is modified oxidatively with the conversion of a single histidine residue to asparagine and a single arginine residue to glutamine semialdehyde near the two metal-binding sites on the enzyme. Alkaline proteinases of *Escherichia coli* effect rapid degradation of the oxidized glutamine synthetase, but have no effect on unoxidized forms (*2,20,21*).

Various MCO systems have been investigated in which fragmentation of the polypeptide chains were observed. Dipeptides of collagen were cleaved when mixed with hydrogen peroxide and Cu(II) ion, along with the production of ammonia (*22*). Upon exposure to hydrogen peroxide, 90% of the histidine residues of a mucus glycoprotein were destroyed, resulting in fragmentation of the polypeptide chain at the effected residues (*23*). Though initially resistant to free radical damage, lenticular proteins were degraded by hydroxyl radicals when the proteins were first cleaved by treatment with cyanogen bromide (*24*). Thus three-dimensional structure of the protein may be important in determining the ability of MCO systems to cause oxidative damage. Site-specific cleavage was demonstrated when Cu, Zn superoxide dismutase was exposed to hydrogen peroxide (*25*). Fragmentation initially occurred between the Pro^{62}- His^{63} residues, followed by random cleavages. His^{63} is coordinated to both Cu(II) and Zn(II). Exposure to catalase blocked both specific and random cleavage types, while use of EDTA blocked only the random cleavages.

Modification of Proteins

Most of the behavior of ROS was discovered by studying the damage produced by ionizing radiation. All amino acids are modified upon exposure to ionizing radiation. In

experiments by Garrison (*26*), Swallow (*27*), and Schussler and Schilling (*28*), the following interactions were revealed:

(1) *Peptide Bond Cleavage*

Ionizing radiation of aqueous solutions produces hydroxyl radicals which are then used to extract hydrogen atoms from the α-CH(R) group of a polypeptide, producing an alkyl radical (Scheme **I**)(*5*):

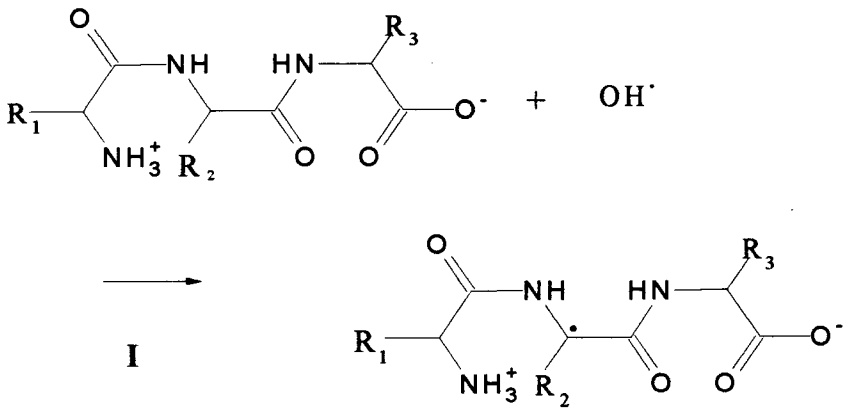

This alkyl radical may react with oxygen to form an alkylperoxy radical (Scheme **II**) or cross-link with another alkyl radical (Scheme **III**)(*5*):

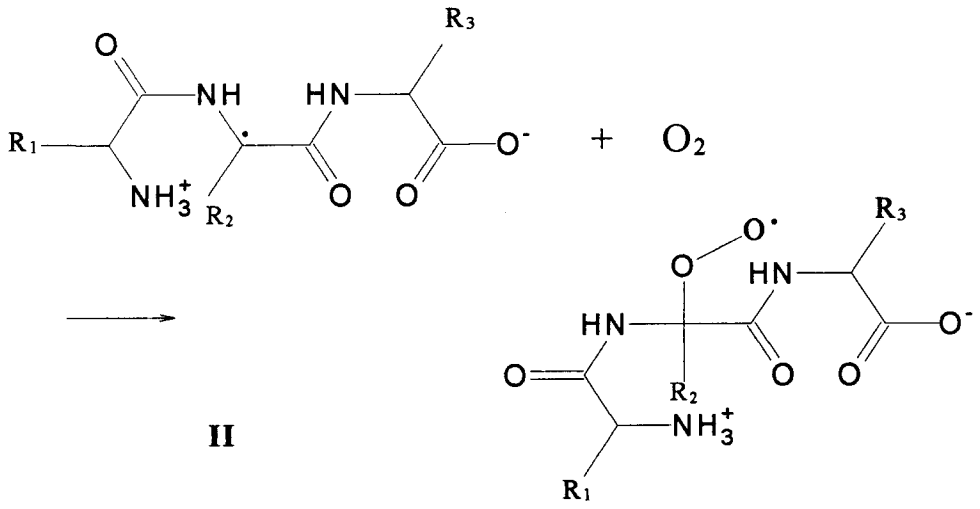

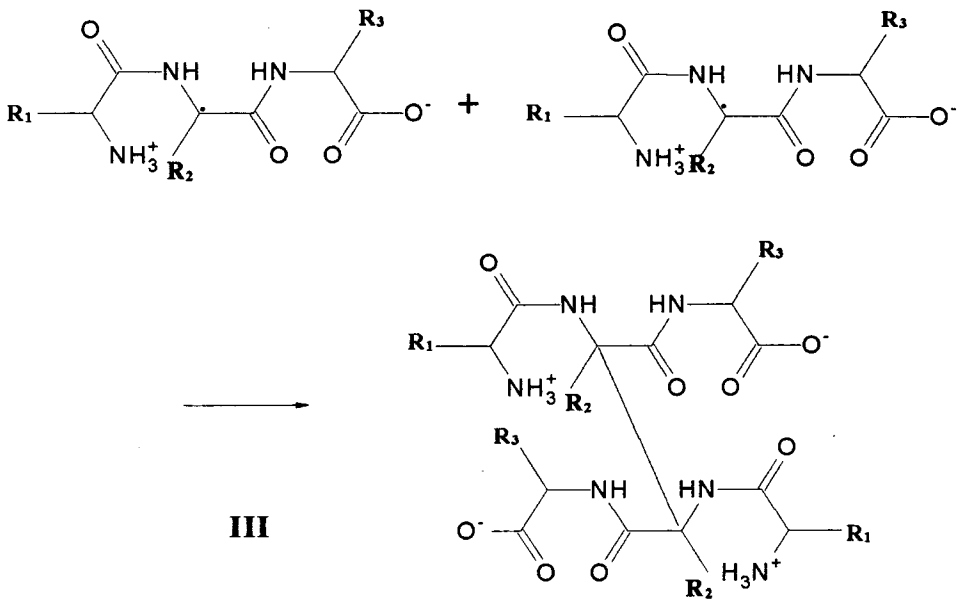

III

Reaction of the alkylperoxy radical with free peroxy radical will form an alkyl peroxide [$H_2NC(R_1)HCONHC(R_2)(\underline{\mathbf{OOH}})CONHC(R_3)HCOO^-$]. Further reaction of this peroxide with either Fe(II) or more free peroxy radical produces an alkoxy protein derivative [$H_2NC(R_1)HCONHC(R_2)(\underline{\mathbf{O^\bullet}})CONHC(R_3)HCOO^-$]. A hydroxy derivative can then be produced via reaction with Fe(II) and H^+: [$H_2NC(R_1)HCONHC(R_2)(\underline{\mathbf{OH}})CONHC(R_3)HCOO^-$].

Peptide bond scission during exposure to ionizing radiation follows via the α-amidation pathway in which a peptide fragment containing a C-terminal amide group and a fragment containing the N-terminal residue blocked by an α-ketoacyl group are formed (*2*).

$$H_2NC(R_1)HCONHC(R_2)(OH)CONHC(R_3)HCOO^-$$

$$\longrightarrow H_2NC(R_1)HCON=C(R_2)CONHC(R_3)HCOO^- + H_2O$$

$$\longrightarrow H_2\,NC(R_1)HCONH_2 + R_2COCONHC(R_3)HCOO^-$$

In direct contrast to the random oxidation of amino acids by ionizing radiation, MCO causes site-specific damage or modification. Use of Fe(II) and H_2O_2 for oxidation of amino acids results in the formation of NH_4^+, α-ketoacids, CO_2, oximes and aldehydes or ketones containing one less C atom (*29*). Three possible mechanisms have been suggested. In the first mechanism, the amino acid is deaminated to form an α-keto acid (eq 14) followed by complete oxidation to form CO_2 and a carboxylic acid derivative with one less carbon (eq 15).

$$RCHNH_3^+COO^- + H_2O_2 \longrightarrow RCOCOO^- + NH_4^+ + H_2O \quad (14)$$

$$RCOCOO^- + H_2O_2 \longrightarrow RCOO^- + CO_2 + H_2O \quad (15)$$

In the second mechanism, the amino acid undergoes deamination rapidly followed by decarboxylation to form HCO_3^- and an aldehyde with one less carbon (eq 16) followed by further oxidation to a carboxylic acid (eq 17).

$$RCHNH_3^+COO^- + H_2O_2 \longrightarrow RCHO + NH_4^+ + HCO_3^- \quad (16)$$

$$RCHO + H_2O_2 \longrightarrow RCOO^- + H^+ + H_2O \quad (17)$$

The formation of aldehydeoximes was postulated via a third mechanism in which some of the amino acid undergoes decarboxylation (eq 18) followed by the iron-catalyzed decomposition of H_2O_2 (eq 19).

$$RCHNH_3^+COO^- + 2\,H_2O_2 \longrightarrow RCH{=}NOH + CO_2 + 3\,H_2O \quad (18)$$

$$2\,H_2O_2 \longrightarrow 2\,H_2O + O_2 \quad (19)$$

In one study (*30*), it was found that oxidation was stimulated by the existence of bicarbonate ion. In addition, the reactions were dependent on substoichiomietric amounts of several chelators but inhibited by greater concentrations. Major products formed from metal-catalyzed oxidation differed from those generated by ionizing radiation. Oxidation of amino acids by ionizing radiation is prevented by radical scavengers, whereas hydroxyl radical scavengers do not impede MCO.

When exposed to ionizing radiation, the double bonds of aromatic amino acids are the main targets, while deamination at the α-carbon atom is a minor side reaction. Tyrosine and phenylalanine oxidation produced mainly mono- and di-hydroxyphenylalanine derivatives (*30*). During MCO, both aromatic and aliphatic amino acids undergo deamination and decarboxylation as shown in eq. 12, 13 and 14. Amino acids have been suggested to be involved in antioxidant defense through their ability to sequester metal ions. Their presence may be an important factor in the protection of proteins, lipids and nucleic acids from oxidative damage.

(2) Oxidation of Amino Acid Residue Side Chains

The side chains of many amino acids are sites of attack by ROS produced by MCO systems. For example, histidine is converted to 2-oxohistidine, 4-OH-glutamate, aspartic acid and asparagine (*31*). Tyrosine can be converted to 3,4-dihydroxyphenylalanine, or form Tyr-Tyr cross-links or 3-nitrotyrosine (*32*). Proline residues are altered to glutamic acid residues; methionyl residues are converted to methionine sulfoxides; cysteine residues to disulfide conjugates; and amino acids are likely converted to carbonyl derivatives (*31*).

One possible mechanism for the site-specific oxidation of a protein was presented by Stadtman in 1990 (*2*). In the model below (Figure 2), Fe(II) binds to the ε-amino group of a lysyl residue to form an Fe(II)-protein coordination complex. Upon reaction with hydrogen peroxide, $OH^{\bullet}$, OH^{-} and an Fe(III)-protein complex is produced. The

newly formed $OH^{\bullet}$ then removes a hydrogen atom from the carbon of the ε-amino group, forming a carbon-centered radical. The unpaired electron of the carbon radical is immediately donated to the Fe(III) to regenerate the Fe(II)-protein complex. The lysyl residue is thought to be converted to an imino derivative and upon hydrolysis, yields an aldehyde derivative and ammonia. The metal binding site would no longer exist, freeing Fe(II) from the protein. The process is perceived as "cage-like", preventing its inhibition by free-radical scavengers.

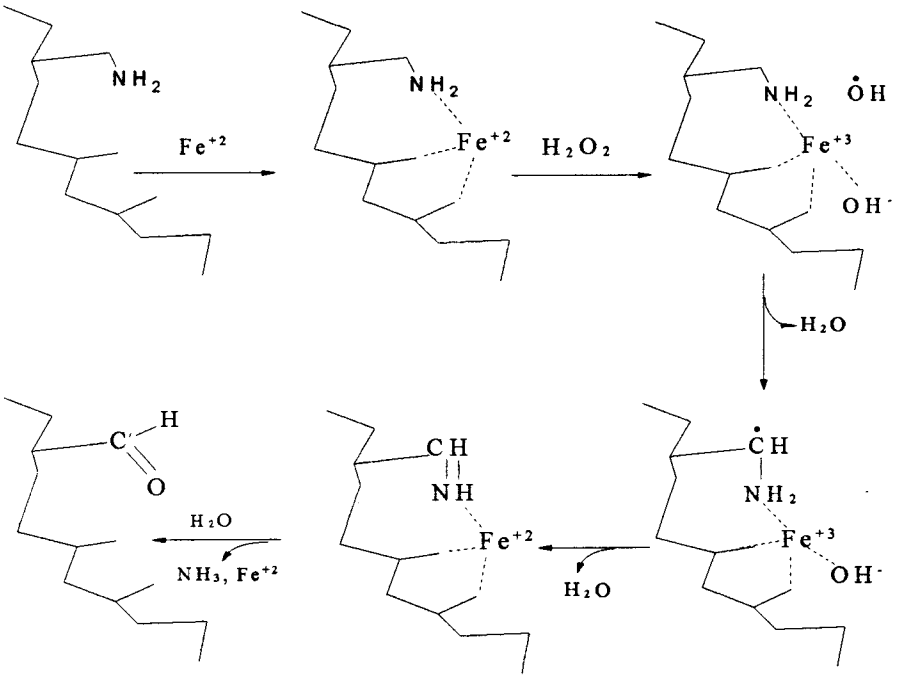

Figure 2 Site-Specific Oxidation of a Protein (2)

(3) Carbonyl Derivatives

Peptide fragments are formed when the main polypeptide chain is cleaved oxidatively as already discussed. In addition, carbonyl groups can be formed via Michael addition reactions when 4-hydroxy-2-nonenal (a lipid peroxidation product) reacts with

lysine's ε-amino group, histidine's imidazole moiety, or cysteine's sulfhydryl group (Scheme **IV**), producing an aldehyde or ketone derivative (*32*).

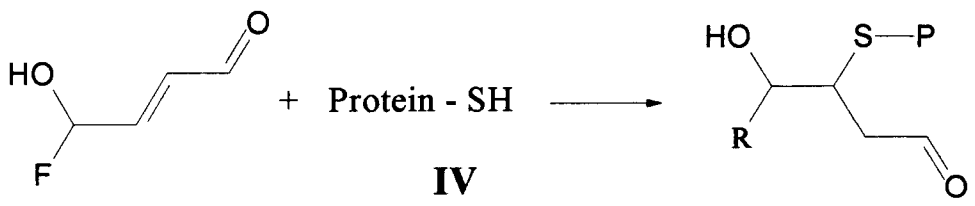

IV

The process of glycation may also introduce carbonyl groups into proteins when oxidized sugar products react with the ε-amino group of lysine (*33*). Thus, the level of carbonyl groups can be used to measure oxidative protein damage.

(4) Cross-linking Reactions

Cross-linking reactions occur between two proteins when induced by ROS. For example, oxidation of cysteine's sulfhydryl groups forms disulfide cross-links; linking of carbonyl groups formed by the oxidation of amino acids in one protein with an ε-NH_2 group of lysine on another protein, and carbon-carbon cross-links can occur between carbon-centered radicals of two amino acids on different proteins (*5*). Formation of cross-linked complexes are believed to cause the accumulation of oxidized proteins as found in aging and some diseases. Cross-linked proteins can accumulate since they are resistant to degradation (*34*).

CHAPTER 2

STATEMENT OF PROBLEM

This research investigates the metal-catalyzed oxidation (MCO) of proteins using dipeptides as model compounds. Examination of the interaction of various metal ions (e.g. Fe(II), Cu(II), Co(II), Ni(II)) with hydrogen peroxide to investigate the site-specific nature of oxidation was pursued. The Fenton reaction (eq 4) can be used to generate ROS at temperatures and pH values that will not denature a protein. Perhaps this method can be used to achieve site-specific cleavage of the polypeptide chain with various metal ions or it may serve as a probe for three-dimensional structure.

The first stage of the research focused on possible cleavage sites using a variety of dipeptides. Dipeptides of the sequence glycyl-X, where X is a number of different residues, were employed as model systems. The hydroxyl radical was produced by the addition of H_2O_2 to Fe(III) . Ultraviolet studies of the dipeptides indicated changes caused by the production of the hydroxyl radical while use of thin layer chromatograpy indicated alterations of the dipeptides. Ideal conditions of pH, temperature and metal cation was also investigated with successful dipeptide fragmentations.

In the second stage, different metal ions were investigated for their effectiveness in the production of reaction products upon addition to dipeptides found to be modified in step one. Various concentrations of metal ion and H_2O_2 were used to determine optimum reaction concentrations with these same dipeptides. TLC comparisons of the products with the standards enabled determination of ideal amounts.

Reversed-phase HPLC was used to separate reaction products and determine possible identification via their retention times in the third stage. HPLC chromatograms were viewed in the far UV where amino acids, carboxylic acids and peptide bonds absorb. Investigation of optimum conditions for the best separation included, but was not limited to: temperature and flow rate effects, and selection of solvent suitable for identification and separation of all fragments.

Upon isolation and separation of resulting fragments through HPLC, collection of the individual products processed through HPLC was then pursued. Sample purity was monitored via HPLC and possible product identification through comparisons between the sample and known standards.

The final stage of the research focused on purification of the HPLC samples. Upon successful isolation, purified samples were prepared for characterization through nuclear magnetic resonance (NMR) and/or mass spectrometry.

CHAPTER 3

THEORETICAL BACKGROUND

Cleavage of the peptide bond using ROS is the focus of this research. Isolation of the resulting products for identification was a major focus of the project. A theoretical review of the principles concerning the separation and collection of fragments is presented in this chapter.

Most biological molecules require liquid chromatography for analysis since such materials are not easily volatilized due to their high molecular weight, polarity, existence of ionic groups, or instability at high temperatures. The sample to be separated is dissolved in a liquid known as the mobile phase. The solution is then passed through a column containing a porous solid matrix known as the stationary phase. The individual components of the sample interact to different extents with the stationary phase, causing varying rates of migration for each component through the matrix. Those components with low affininties for the stationary phase will move through the column faster than those with high affinities. The interactions depend upon the nature of the solute being separated and the choices of mobile and stationary phases.

Thin-Layer Chromatography

A variation of paper chromatography, thin layer chromatography (TLC) places a thin coating of solid material on a solid support as the stationary phase. A tiny sample of the mixture to be separated is applied to one end of the plate. Standing the lower edge of

the plate (below the spot) in a solvent mixture of organic and aqueous components allows the solvent to move up the plate by capillary action.

The solubilities of the sample's components in the mobile phase determines their rates of migration. The rate of migration of one component can be calculated as the R_f value (eq 20). Each substance will have a characteristic R_f in a particular solvent.

$$R_f = \frac{\text{distance traveled by a component}}{\text{distance traveled by solvent front}} \qquad (20)$$

To visualize α-amino acids, the chromatogram is sprayed with a reagent which reacts to form a colored compound. Ninhydrin reacts with α-amino acids in a multi-step reaction to produce the compound "Ruheman's purple" (*33*) (Scheme **V**) Deamination of the amino acid prevents its detection by ninhydrin, as will modification such as acetylation.

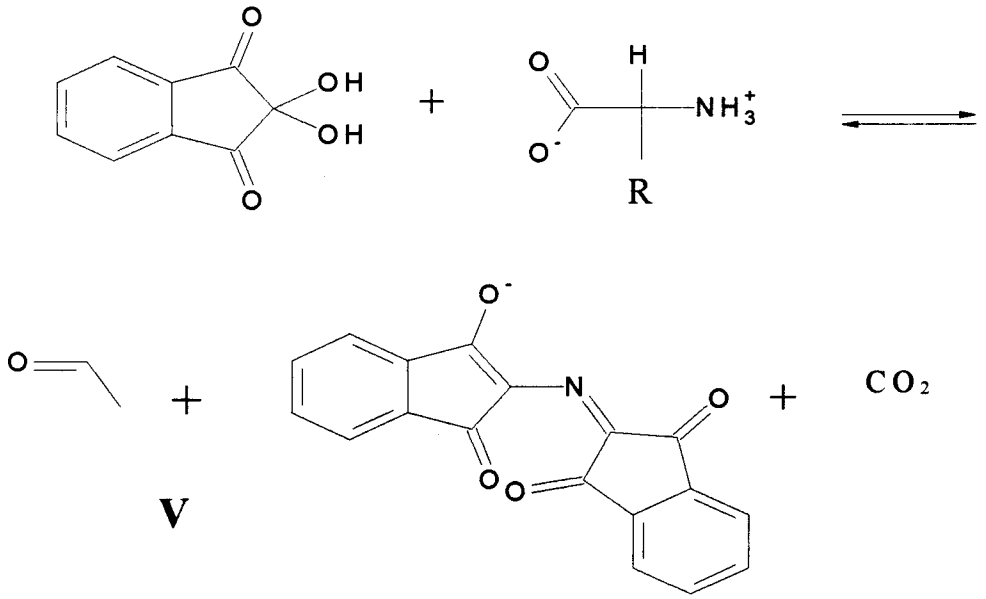

V

Reversed-Phase High Performance Liquid Chromatography

First used in the 1960s, high performance liquid chromatography (HPLC) is distinquished from conventional liquid chromatography by using high efficiency columns, sophisticated instruments and very sensitive detectors. In return, greater resolutions, faster speeds, better recovery and greater sensitivities are obtained.

The use of a liquid system requires much higher operating pressures and consequently much lower diffusion rates than gas chromatography systems. In order to keep the total time for analysis reasonable, short columns and small particle sizes have been developed.

HPLC permits analysis of non-volatile, thermally labile compounds. This technique uses solvent under high pressure to elute the column. The pump must maintain a constant flow of solvent such that no surges in pressure occur. Solvents must be pure and require degassing prior to introduction to the system. Any air bubbles formed can upset the steady pressure state.

The separation of amino acids by reversed-phase HPLC typically used a sulfonated polystyrene ion exchanger resin. Amino acids were detected by reaction with ninhydrin. In 1951, it took 6 hours for Moore and Stein to separate 20 amino acids in the original system (*35*). Reported separations of 30 minutes to one hour were eventually obtained with the use of higher pressures and smaller polystyrene particle sizes. Some problems associated with such soft resins are compaction under high pressures and a decrease in their porosities when in contact with organic solvents.

Isocratic separations involve a constant ratio of components in the solvent mixture whereas gradient elutions use varied ratios. Samples are loaded onto the column by an injection system that allows for constant flow of solvent. The column is made of stainless steel and packed with stationary phase containing tiny spherical particles, 5-10 micrometers in diameter. Such small size particles permit equilibration between the

external solvent and the solvent of the particle's matrix. The development of silica particles, as small as 5-10 micrometers, provided mechanical stability with pressures up to 5000 psi and no swelling in organic solvents (*35*). Silica particles also have higher rates of diffusion which permit more efficient separations. The packing materials of the HPLC's stationary phase is usually made of silica or polymers and are known as the support matrix. These two materials have different physical and chemical properties which can provide for a wide range of interactions that ultimately provide a means of separation for a sample. Different types of ligands can be covalently attached to the support matrix.

Selection of the column depends upon the types of molecules to be separated. Affinity chromatography is used to purify biologically active molecules. A specific ligand which can noncovalently bind to the impure protein is covalently attached to the matrix. As the sample passes over the matrix, the protein attaches to the ligand and is thus removed from the rest of the mixture. The desired protein can later be detached from the ligand-matrix complex by altering the make-up of the eluent (*36*).

Adsorption chromatography separates molecules according to their partition between a polar column material and a nonpolar solvent. Molecules to be separated adsorb to the insoluble surface through van der Waals or hydrogen bonding interactions (*36*). Macromolecules, such as enzymes and nucleic acids, can be separated by hydroxylapatite chromatography, which is dependent upon the degree of binding to calcium or phosphate sites on a matrix (*36*). Size exclusion chromatography separates molecules according to their size and shape and can be used to estimate molecular mass (*36*). In ion exchange chromatography, ions in solution replace ions that are bound to an insoluble matrix. Normal phase chromatography relies on the varying polarities of molecules for separation. For example, very polar molecules interact strongly with the silica particles that make up the support matrix and will have longer retention times.

In HPLC, retention times on the column are decreased by forcing solvent through the column with pressures up to 10,000 psi (*36*). Methods for separation may include

adsorption, ion exchange, size-exclusion or reversed-phase chromatography. The column consists of a long, narrow tube packed with small beads coated with a thin layer of stationary phase. The mobile phase is determined by the separation method selected.

On the other hand, reversed-phase chromatography will separate molecules based on their hydrophobicity. The stationary phase is a nonpolar liquid on an inert solid, while the mobile phase is a polar liquid. Polar molecules will weakly interact with the matrix and elute quickly. This method is particularly suitable for separation and analysis of amino acids, which tend to be insoluble in most organic solvents. The three groups of amino acids (acidic, neutral, and basic) are separated from each other by their major ionic interaction with the stationary phase. However, amino acids within these groups are separated by hydrophobic, van der Waals and aromatic π-π interactions (*35*).

Silica particles maximize the hydrophobicity of the solid. Weakly acidic silanol groups can pose a problem for the basic amino acids. Using a buffered mobile phase can negate these interactions (*35*).

Since the polar amino acids have a very small retention time, there is usually insufficient resolution within this group. Hancock and Harding suggest several modifications: (*35*)

1) Derivatizing the amino or carboxyl group will remove the zwitterionic form of the amino acid.

2) Addition of a nonpolar anionic ion-pairing reagent such as alkylsulfates or sulfonates should increase the retention and selectivity of the separation.

Variations in pH and temperature can have major impact on the order and amount of retention of amino acids. Flow rates for analytical HPLC columns are typically 0.5 - 1.0 ml/min. Separated amino acids can be monitored by ultraviolet (UV) spectroscopy, refractive index or by fluorescence detection. The solvents used cannot have absorptions in the UV region being analyzed. The great advantages to HPLC include high resolutions,

short analysis times, high sensitivities and ability to automate; disadvantages include its small capacity and high price (*36*).

Mobile Phase

The choice of mobile phase is critical to the success of amino acid separations. Not only must the solvent be transparent at low wavelengths, it must be suitable for use with the HPLC instrumentation and the support phase of the column.

Using only one set of conditions for the mobile phase to separate amino acid peptides is not expected to be successful due to the large range of polarities. Most separations involved the nonpolar amino acids which show the best retention on reversed-phase columns (C_{18}). Mobile phases often contained low concentrations of a phosphate or acetate salt, at low pH. The addition of a salt to a reversed-phase column's mobile phase can aid in blocking the interactions of the silanol groups in the packing material with the peptide samples. Phosphate salts or phosphoric acid permits UV detection from 200-220 nm (*37*). The polar $H_2PO_4^-$ anion pairing with the cationic RNH_3^+ of a peptide increases the polarity of a hydrophobic peptide.

Polar amino acids, with very short retention times in the systems described, were not successfully resolved. Hydrophobic ion-pairing reagents, on the other hand, can be used to increase the retention of the polar peptides (*37*). Alkyl sulfonates added to the mobile phase are often cited as such reagents. Perfluoroalkanoic acids can be used for polar peptides as well (*38*).

CHAPTER 4

EXPERIMENTAL

The experimental work will be presented in 4 stages as follows:

Stage 1: Initial Screening of Dipeptides

Stage 2: Various Metal Ions

Stage 3: Analysis of Reaction Products by HPLC

Stage 4: Separation of GY(24) through Other Chromatographic Techniques

In Stage 1, initial screening using dipeptides of the form glycyl-X (X being tyrosine, histidine, methionine, glycine, glutamine, phenylalanine, proline, serine and tryptophan) in addition to alanyltyrosine, prolyltyrosine and tyrosylglycine were exposed to the hydroxyl radical using Fe(III) and H_2O_2. Ultraviolet spectra of each dipeptide sample after 24 hours incubation were compared to their respective standards. Thin layer chromatography was used to monitor any changes in the dipeptide. Ammonia production for several reactions was monitored by the reductive amination of 2-oxoglutarate to glutamate (eq. 21). The decrease in absorbance at 340 nm, due to the oxidation of nicotinamide adenine dinucleotide phosphate (NADPH), is proportional to the concentration of NH_3 consumed. The reaction is catalyzed by L-glutamate dehydrogenase (GLDH).

$$\text{2-oxoglutarate} + NH_3 + \text{NADPH} \xrightarrow{\text{GLDH}} \text{glutamate} + \text{NADP} \qquad (21)$$

Acetylation of Gly-Tyr was pursued in an attempt to alter the dipeptide. Successfully altered molecules were then exposed to the hydroxyl radical, testing for blockage of any modification caused by reactive oxygen species.

In Stage 2, the effects of pH, temperature and various metal ions were used to examine rates of modification for those dipeptides reacting favorably in Stage 1.

Investigation of optimum flow rates, temperatures and solvents were studied for maximum separation of reaction products using HPLC in Stage 3.

In Stage 4, separation of Gly-Tyr (after exposure to hydroxyl radical for 24 hours at 37 °C) was pursued using other chromatographic techniques.

Stage 1 Initial Screening of Dipeptides

Materials: glycine (Gly), histidine (His), tyrosine (Tyr), glycylglutamine (Gly-Glu, GE), glycylphenylalanine (Gly-Phe, GF), glycylproline (Gly-Pro, GP), glycylserine (Gly-Ser, GS), glycyltryptophan (Gly-Trp, GW), alanyltyrosine (Ala-Tyr, AY), prolyltyrosine (Pro-Tyr, PY), tyrosylglycine (Tyr-Gly, YG), glycyltyrosine (Gly-Tyr, GY), glycylhistidine (Gly-His, GH), glycylmethionine (Gly-Met, GM), glutamate (Glu), methionine (Met), cysteine (Cys), glycylglycine (Gly-Gly, GG), catalase, and a diagnostic kit to measure ammonia production (catalog number 171-A) were purchased from Sigma Chemical Company, St. Louis, MO; potassium monohydrogen phosphate (K_2HPO_4), potassium dihydrogen phosphate (KH_2PO_4), ethylene diamine tetraacetic acid (EDTA), sodium carbonate (Na_2CO_3), sodium sulfate (Na_2SO_4) and ferric sulfate ($Fe_2(SO_4)_3$) were purchased from J.T. Baker Chemical Company, Phillipsburg, N.J.; hydrogen peroxide (H_2O_2), 1-butanol, glacial acetic acid, hydrochloric acid, petroleum ether, n-propanol, diethyl ether, ethyl acetate, acetic anhydride, phosphoric acid (H_3PO_4), sodium nitrite ($NaNO_2$), sodium bicarbonate ($NaHCO_3$), toluene and ammonia were purchased from Fisher Scientific, Fairlawn, NJ; L-glutamate dehydrogenase enzyme

(GLDH) and potassium hydroxide (KOH) were purchased from Eastman Kodak Company, Rochester, NY; sodium hydroxide (NaOH) was purchased from V.W.R. Scientific, West Chester, PA; pyridine, carbobenzoxy chloride, ninhydrin, hydroxylamine and acetone were purchased from Aldrich Chemical Company, Milwaukee, WI; sodium acetate and sulfanilic acid were purchased from Mallinckrodt, St. Louis, MO. All solutions were prepared using deionized water. 20 x 20 cm linear K-preadsorbent 60 Angstrom silica gel TLC plates, 250 μm thickness, were obtained from Whatman Co., Kent, England. TLC chambers were purchased from Analtech, Newark, DE.; microcentrifuge tubes were purchased from Simport Co., Quebec, Canada.

Instrumentation: Ultraviolet spectral data were obtained using a Hewlett Packard diode array spectrophotometer model 8452 A; an Isotemp Water Bath by Fisher was used to incubate samples; and a Buchi rotary evaporator (R-114) was used to remove non-aqueous solvent from samples.

SAMPLE PREPARATION

Exposure to Hydroxyl Radical

Amino acids and dipeptides were prepared at a concentration of 5 mM and buffered at pH 6.8, using 10 mM potassium phosphate (KPi) buffer. Metal ion was added in a 1:2.5 molar ratio with the buffered dipeptides. After five minutes of equilibration at room temperature, H_2O_2 was added in a 20-fold molar excess. Controls were run using dipeptide alone (GXC), dipeptide and H_2O_2 (GXP), and dipeptide with metal ion (GXFe). Each trial contained the following solutions placed into separate microcentrifuge tubes.

- GXC (500 μL of 5 mM GX, 500 μL of deionized H_2O, where X was His, Met, Tyr, Gly, Phe, Pro, Ser, Trp, Cys or Glu)
- GXFe (500 μL of 5 mM GX, 200 μL of 5 mM $Fe_2(SO_4)_3$, 300 μL of deionized H_2O)

- GXP (500 μL of 5 mM GX, 250 μL of 200 mM H_2O_2, 250 μL of deionized H_2O)

- GX (500 μL of 5 mM GX, 200 μL of 5 mM $Fe_2(SO_4)_3$, 250 μL of 200 mM H_2O_2, 50 μL of deionized H_2O)

Samples were incubated at 37 °C for 24 hours. 100 or 200 μL aliquots were removed at timed intervals and the reaction stopped by the addition of 10 μL of catalase (1 mg/mL in 10 mM KPi buffered at pH 6.8).

Variations in Sample Preparation

In order to investigate the possibility of metal contamination in a particular trial of Gly-Met with peroxide, KPi buffer was made 5 mM in EDTA. A subsequent drop in the buffer's pH required addition of 2 M NaOH to return the pH to 6.81.

UV SPECTRA

Dipeptides exposed to free radicals were prepared using 200 μL of the incubated sample with 2.8 mL KPi. Spectra were run on the test samples, followed by a comparative analysis on the standard dipeptide, GX(std) (using 100 μL of 5 mM standard with 2.9 mL KPi) and the amino acid (100 μL 5 mM amino acid with 2.9 mL KPi).

THIN LAYER CHROMATOGRAPHY

General TLC Development

Silica gel TLC plates were prepared by heating at 100 °C for 30 minutes. The TLC chamber was equilibrated by placing 30 mL of selected solvents into the chamber along with a saturation pad coated with solvent for 2-3 hours before the plates were inserted.

Lanes on the TLC plate were spotted with amino acid standards, dipeptide controls, and dipeptides after exposure to free radicals. Plates were developed for

approximately 6 hours. Ninhydrin solution (0.2% (w/v) in 1-butanol) was used to visualize the standards and the reaction products.

AMMONIA ASSAY

Gly-Tyr standard (5 mM) and Gly-Tyr incubated with hydroxyl radical for 3, 6 and 24 hours were prepared. Catalase (10 μL) was added to 250 μL of the incubated samples to stop the reaction. The ammonia assay solution was reconstituted as directed by the product's preparation instructions. One milliliter cuvets were prepared as follows:

- Blank (1000 μL assay solution, 100 μL H_2O)
- Control (1000 μL assay solution, 100 μL NH_3 control solution)
- Test 1 (1000 μL NH_3 assay solution, 100 μL GYC)
- Test 2 (1000 μL NH_3 assay solution, 100 μL GY_3)
- Test 3 (1000 μL NH_3 assay solution, 100 μL GY_6)
- Test 4 (1000 μL NH_3 assay solution, 100 μL GY_{24})

After 3 minutes equilibration, 10 μL GLDH enzyme solution was added to each cuvet. An absorbance spectrum was run at 340 nm before and after GLDH was added.

In an attempt to chelate the Fe(III) ion (which may inhibit the GLDH enzyme), 3.5 mL of 2 mM EDTA was added to the ammonia assay solution during reconstitution. Gly-Tyr and Gly-His were prepared as above, followed by testing with the ammonia assay/EDTA solution. Spectra were run on these solutions as well as their respective samples incubated with hydroxyl radical after 3, 6, and 11 hours.

ACETYLATION OF GLY-TYR

Acetylation of the phenolic hydroxyl residue in Gly-Tyr was carried out as described by Shaltiel and Patchornik (*39*). A solution made 20 mM in Gly-Tyr and 0.02 M in $NaHCO_3$ was buffered to pH 7.48. A ten-fold molar excess (200 mM) of acetic anhydride was added. The sample was monitored by TLC by spotting treated dipeptide

and the standard every 30 minutes for a total of 90 minutes. The solvent for the TLC was 70:30 (v/v) n-propanol:deionized water.

Samples of Gly-Tyr(std) and Gly-Tyr treated with acetic anhydride were prepared for UV spectroscopy (200-320 nm), using $NaHCO_3$ as the blank. To strengthen the signal, trials were run with 5 mM, 20 mM and 100 mM concentrations of dipeptides.

An alternative method for acetylation, using a different buffer, involves the addition of acetic anhydride prepared with 1.0 M sodium acetate at pH 5.8 (*40*). 100 mM Gly-Tyr was treated with a 20-fold molar excess concentration of acetic anhydride. The reference sample contained sodium acetate buffer, but no acetic anhydride. UV spectra were observed over a 1 hour period from 274-284 nm to calculate the % acetylation over time. Using 70:30 (v/v) n-propanol:water solvent, TLC was performed on Gly-Tyr samples prepared in the previous step. Very faint spotting on the TLCs could indicate a very low percentage acetylation. To increase the percentage, acetic anhydride was added first in a 530-fold, then a 2000-fold molar excess to Gly-Tyr samples. UV spectra were observed on the samples from 220-340 nm.

REVERSING ACETYLATION OF GLY-TYR

In an attempt to reverse any acetylation of the phenolic hydroxyl residue in Gly-Tyr by acetic anhydride, hydroxylamine (NH_2OH-HCl) was added to 5 mM acetylated Gly-Tyr (AGY) first in a 2-fold, then a 10-fold molar excess. TLCs on samples were run in 70:30 (v/v) n-propanol:water solvent.

MASKING THE N-TERMINUS OF GLY-TYR

Acetylation of the hydroxyl group of tyrosine may be simultaneously accompanied by acetylation of the N-terminus of glycine. To prevent this possibility, an attempt to mask the α-amino function of the dipeptide prior to acetylation was undertaken. A

modified version of the Schotten-Baumann procedure was used to prepare a carbobenzoxyamino acid (CBZ-GX) (*41*).

A solution was prepared using 10 mmol Gly-Tyr diluted to 30 mL with 2.00 M $NaHCO_3$ solution. 4.00 M NaOH was used to maintain a pH of 10. A total of 1.6 mL (11.0 mmol) carbobenzoxy chloride was added dropwise to the Gly-Tyr solution and stirred mechanically at room temperature for 3 hours. The reaction mixture was extracted twice with 35 mL portions of diethyl ether. The aqueous layer was acidified to pH 2 with 5 M HCl. The resulting oil was extracted with three 40 mL portions of ethyl acetate, the organic layer saved and the aqueous bottom layer recycled with fresh ethyl acetate. The ethyl acetate layer was dried over anhydrous sodium sulfate. After filtering, this layer was concentrated via rotary evaporation. Crystallization of the remaining oily liquid was attempted by extraction with diethyl ether and addition of petroleum ether. The very sticky material adhering to the inside walls of the flask was redissolved by dropwise addition of ethyl acetate. The cloudy solution was evaporated in a fume hood, producing the same residue as found following rotary evaporation.

The following solvent pairs were investigated to attempt crystallization: acetone-petroleum ether, diethyl ether-petroleum ether, and toluene-petroleum ether. Of these three, the toluene-petroleum ether produced the most promising results and was used on the entire oily sample. TLC of CBZ-Gly-Tyr was compared to the Gly-Tyr standard using 70:30 (v/v) n-propanol:deionized water solvent. Ninhydrin was initially used as the developing reagent, followed by use of Pauly Reagent in a second run. Pauly Reagent consists of 10 mL 5% sodium nitrite added to 1 mL of 0.9% sulfanilic acid in 1.0 M HCl. Plates sprayed with Pauly Reagent were then sprayed with a 5% Na_2CO_3 solution.

REDUCING RANDOM OXIDATION OF GLY-TYR

Samples of Gly-Tyr were prepared with the addition of 200 mM D-mannitol, a hydroxyl radical scavenger. To test site-specific damage, mannitol was added to the reaction mixtures in various ratios:

-500 μL GY, 150 μL mannitol, 150 μL H_2O_2, 200 μL Fe (III)

-500 μL GY, 150 μL mannitol, 150 μL H_2O_2, 150 μL Fe (III)

-500 μL GY, 100 μL mannitol, 100 μL H_2O_2, 200 μL Fe (III)

-500 μL GY, 50 μL mannitol, 50 μL H_2O_2, 200 μL Fe (III)

-500 μL GY, 100 μL mannitol, 100 μL H_2O_2, 100 μL Fe (III)

-500 μL GY, 50 μL mannitol, 50 μL H_2O_2, 50 μL Fe (III)

TLC of all samples were run with 70:30 (v/v) n-propanol:deionized water solvent on silica gel chromatographic plates. UV using 50 μL samples and 1500 μL deionized water were run from 200-320 nm .

Stage 2 Various Metal Ions

Materials: glycyl-tyrosine (Gly-Tyr, GY), alanyl tyrosine (Ala-Tyr, AY), prolyl tyrosine (Pro-Tyr, PY), glycine (Gly), tyrosine (Tyr), alanine (Ala), proline (Pro), catalase and murexide were purchased from Sigma Chemical Company, St. Louis, MO; potassium monohydrogen phosphate (KH_2PO_4) and potassium dihydrogen phosphate (KH_2PO_4) were purchased from J.T. Baker Chemical Company, Phillipsburg, NJ; copper (II) sulfate pentahydrate ($CuSO_4 \cdot 5\ H_2O$), iron (II) sulfate ($FeSO_4$), 1-butanol, hydrogen peroxide (H_2O_2), n-propanol, nickel (II) nitrate hexahydrate [$Ni(NO_3)_2 \cdot 6\ H_2O$] and cobalt (II) nitrate hexahydrate [$Co(NO_3)_2 \cdot 6\ H_2O$] were purchased from Fisher Scientific, Fairlawn, NJ; ninhydrin was purchased from Aldrich Chemical Company, Milwaukee, WI.

Instrumentation: High Pressure Liquid Chromatography analysis was performed on an IBM LC/9533 ternary gradient with a reverse phase C18 Alltima 5-micron analytical

column (250 mm x 4.6 mm) by Alltech Associates, Deerfield, IL; samples were incubated in a Fisher Isotemp Waterbath. Injections were made with a 100 µL syringe from Hamilton company, Reno, Nevada; and TLC chambers were purchased from Analtech, Newark, DE.

SAMPLE PREPARATION AND COMPARISONS WITH COPPER (II), NICKEL (II), COBALT (II) AND IRON (II)

Amino acids and dipeptides were prepared at a concentraion of 5 mM and buffered at pH 6.8, using 10 mM KPi (as prepared in Stage 1). 5 mM solutions of $CuSO_4 \cdot 5\ H_2O$, $Ni(NO_3)_2 \cdot 6\ H_2O$, $Co(NO_3)_2 \cdot 6\ H_2O$ and $FeSO_4$ were prepared and added to the buffered dipeptides in a 1:2.5 molar ratio. After 5 minutes, H_2O_2 was added to the metal ion-dipeptide complex in a 20-fold molar excess. Controls were run using dipeptide alone, dipeptide and H_2O_2, and dipeptide and metal ion alone. Dipeptides tested were Gly-Tyr, Ala-Tyr, and Pro-Tyr with Cu(II) and Gly-Tyr with Fe(II).

Samples were incubated at 37 °C in a water bath for 24 hours. The reaction was stopped by the addition of 50 µL of catalase solution (1 mg catalase/mL KPi buffer).

Using 70:30 (v/v) n-propanol:deionized water solvent, TLC was performed on samples and the results were visualized with ninhydrin.

Spectra were run from 200-320 nm on the GY(24), AY(24) and PY(24) samples along with their standards.

Although catalase stops the activity of H_2O_2, the existence of other free radicals produced during the reaction could continue to modify the products. Using the Cu(II) samples prepared above, 15 mM murexide was added (1:4 molar ratio) to detect the presence of radicals after reaction. Spectra were run from 430-630 nm. 100 µL of samples were added to 2.90 mL deionized water, whereas 50 µL of standards were added to 2.95 mL deionized water. Deionized water was used as the blank.

Stage 3 Analysis of Reaction Products by HPLC

Levin and Grushka (*42*) separated underivatized amino acids using a mobile phase containing copper (II) and an alkyl sulfonate. Copper (II) forms a complex with carboxylate that absorbs at 235 nm.

Materials: sodium acetate (NaAc) was purchased from Mallinckrodt, St. Louis, MO; glacial acetic acid (HAc), hydrogen peroxide (H_2O_2), 1-propanol and 1-butanol were purchased from Fisher Scientific Fairlawn, NJ; copper (II) acetate [$Cu(C_2H_3O_2)_2$], ethylene diamine tetraacetic acid (EDTA), potassium monohydrogen phosphate (K_2HPO_4), potassium dihydrogen phosphate (KH_2PO_4), D-mannitol, iron (III) sulfate [$Fe_2(SO_4)_3$], methanol and acetonitrile were purchased from J.T. Baker Chemical Company, Phillipsburg, NJ; sodium 1-heptanesulfonate was purchased from Alltech Associates, Deerfield, IL; heptafluorobutyric acid (HFBA) and ninhydrin were purchased from Aldrich Chemical Company, Milwaukee, WI; glycyltyrosine (Gly-Tyr, GY), glycine (Gly), tyrosine (Tyr), catalase and murexide were purchased from Sigma Chemical Company, St. Louis, MO; helium gas was purchased from Gas Technics, North Royalton, OH; and 20 x 20 cm linear K-preadsorbent 60 Angstrom silica gel TLC plates, 250 μm thickness, were obtained from Whatman Co., Kent, England.

Instrumentation: High pressure liquid chromatography analysis was performed on an IBM LC/9533 ternary gradient with a reverse phase C18 Altima 5-micron analytical column (250 mm x 4.6 mm) by Alltech Associates, Deerfield, IL, and on a Perkin-Elmer Series 400 Liquid Chromatograph with LC-75 Spectrophotometric Detector; TLC chambers were purchased from Analtech, Newark, DE; centrifugation was performed with a Beckman E Centrifuge, Palo Alto, CA; and injections were made with a 100 μL syringe purchased from Hamilton Company, Reno, Nevada.

COPPER (II)/ALKYLSULFONATE MOBILE PHASE

Solvent Preparation

Acetate buffer at pH 5.6 was prepared using 1.2 mM acetic acid (HAc) and 8.8 mM sodium acetate (NaAc). Solvent was made to be 10 mM in the acetate buffer, 0.5 mM in copper (II) acetate and 5 mM in heptanesulfonate. Solvent was filtered and degassed prior to its use for HPLC analysis. A minimum of 30 minutes equilibration was required. Solvent was sparged with helium. Once a week, the HPLC column was washed with 0.01 M EDTA in the 0.1 M acetate buffer prepared above.

Operating Parameters

Samples to be injected were first microcentrifuged and filtered with Millipore Ultrafree-MC filters. The wavelength was set at 235 nm, and runs were 20 minutes long.

The following standards were tested:

- 100 μL injections of 5 mM Gly-Tyr and Gly at room temperature at a flow rate of 1.0 mL/min and then 2.0 mL/min.
- 100 μL injections of 5 mM Tyr at 30 °C and a flow rate of 1.2 mL/min.
- 20 μL injections of 0.5 mM Gly-Tyr, Gly and Tyr at 30 °C and 1.2 mL/min flow rate.
- 40 μL injections of 0.5 mM Gly-Tyr(24) at 30 °C and 1.2 mL/min flow rate.

TLC

Eluent from the HPLC was collected by monitoring their detection signal. The eluent was spotted on TLC plates in 70:30 (v/v) n-propanol:water solvent to verify the identity of each sample.

UV Spectroscopy

In an attempt to find the lowest concentration of sample which can be detected via UV, various size volumes of 0.5 mM Tyr were injected into the HPLC, followed by UV spectroscopy of the sample from 200-320 nm using the Waters 990 UV spectrophotometer attached to the HPLC. The sample had to be small enough to not

overload the HPLC, but large enough for its signal to be detected by UV or TLC. It was determined that by taking 40 μL of 0.5 mM concentration of samples for injection and collecting 4-5 eluent samples, enough sample was available for UV analysis. Standards for UV comparison were prepared with 250 μL of 0.5 mM standard and 2.75 mL heptanesulfonate buffer.

System Peaks

Levin and Grushka (*42*) refer to system peaks occurring with their solvent system which can mask sample peaks. What the literature refers to as "Peak C" (due to Cu(II)) was found at 2 minutes. To keep this peak from being problematic, all solutes were dissolved in a solution containing the same Cu(II) concentration as the solvent (0.5 mM). System "Peak D", due to the sulfonate ions, was corrected by dissolving solutes in the same concentration as the heptanesulfonate found in the mobile phase.

In an attempt to clear up the system peaks, the heptanesulfonate buffer was used to dilute all the standards from 5mM to 0.5 mM concentrations.

The following trials were run:

- 40 μL injections of Gly in 0.5 mM heptanesulfonate at room temperature for 20 minutes at a flow rate of 1.2 mL/minute

- 40 μL injections of Tyr in 0.5 mM heptanesulfonate for 30 minutes and then 60 minutes at a flow rate of 1.2 mL/minute run at 30 °C, 34 °C, and then 40 °C.

Reducing Retention Times

The concentration of heptanesulfonate was adjusted from 5 mM to 0.8 mM for the mobile phase and all standards were prepared with this new buffer.

The following trials were run:

- 40 μL injections of Gly, Tyr, GYC, and GY(24) at 40 °C for 30 minutes at a flow rate of 1.2 mL/minutes.

Experiments on GY(24) to Resolve Early Eluting Peaks

40 μL injections of GY(24) were run for 30 minutes at a flow rate of 1.2 mL/minute at 30°C and then 40°C. Using 0.8 mM heptanesulfonate allows for a reduction in the very long retention time of Tyr, but the low concentration causes GY(24) peaks to be crowded too closely together to diffferentiate. Increasing the concentration of the alkylsulfonate will retain samples longer on the column, allowing a greater separation of the earlier peaks. The concentration of heptanesulfonate buffer was increased to 2.5 mM and 5 mM and run at 30 °C.

Prevention of GY(24) Deteriorations

The presence of radicals in GY(24) was tested with murexide. To quench radical formation in GY(24), methanol was added and the sample retested. After 48 hours the GY(24) samples with and without methanol were tested again for the presence of radicals.

New Gly-Tyr samples were prepared at 2.5 mM in 10 mM KPi (pH 6.8), then diluted to 0.5 mM with 5 mM heptanesulfonate buffer. The following experiments were run:

- HPLC using 40 μL injections of 0.5 mM GYC, 0.5 mM GY(24), 0.5 mM GY(24) with 200 mM methanol, and 0.5 mM Gly.

- UV from 430-630 nm using 25 μL 15 mM murexide, 100 μL of sample with methanol, and 2.875 mL deionized water run after 24 and then 48 hours of incubation.

- TLC in 70:30 (v/v) n-propanol:water solvent using Gly, GYC, GY(24) and GY(24) with methanol followed by detection with 0.2% (w/v) ninhydrin in n-butanol.

ACETONITRILE MOBILE PHASE

A major problem with the heptanesulfonate mobile phase is removal of the NaAc and heptanesulfonate from the eluent in order to prepare samples for further study, particularly via proton NMR. To alleviate this concern, a 50:50 (v/v) acetonitrile:deionized water solution was used for the HPLC mobile phase, since acetonitrile is easily removed by rotary evaporation. With a flow rate of 1.0 mL/min, 40 μL of 0.5 mM Gly and 0.25 mM GY(24) were injected with detection at 210 nm.

HEPTAFLUOROBUTYRIC ACID with IBM LC 9533 HPLC

Harding, *et al.* (*38*), successfully separated underivatized peptides by reversed-phase HPLC using ether soluble, ion-pairing reagents called perfluoroalkanoic acids. Addition of 5 mM concentrations of these reagents to the mobile phase increased the retention times of amino acids and yet was easily removed by extraction with ether.

Mobile phase was prepared with 5 mM heptafluorobutyric acid (HFBA). The flow rate was set at 1.5 mL/min at room temperature and the eluent was monitored at 210 nm. HFBA is transparent at this wavelength and dipeptide absorptions are stronger at 210 nm than at 234 nm.

The following trials of 15 minute duration were run:

- 50 μL 5 mM Gly

- 50 μL 5 mM GY(std)

- 50 μL 2.5 mM GY(24)

In an attempt to minimize negative system peaks, 50 mM Gly and 50 mM Gly-Tyr in KPi were prepared and then diluted each 1:10 (v/v) with 5 mM HFBA. The Gly-Tyr was incubated with Fe(III) and H_2O_2 for 24 hours at 37 °C. 500 µL of catalase was used to stop the reaction.

In order to stabilize the baseline, a new mobile phase consisting of 5 mM HFBA made with 15% acetonitrile was prepared and and used to dilute 50 mM Gly to 0.5 mM. 50 µL Gly was injected at 1.0 mL/min and the HPLC was run for 15 minutes. Using 5 mM HFBA, the following trials were run at 235 nm for 30 minutes at 1.0 mL/min flow rate while monitoring at 235 nm.

- 50 µL 5 mM Gly

- 80 µL 5 mM Gly

- 100 µL 5 mM Tyr

- 100 µL 5 mM GY(std)

Tests of GY(24) with 5 mM HFBA were run at the conditions listed above. A lower flow rate (0.5 mL/min) was used to obtain a better separation of Gly, Tyr and GY(24). Flow rates of 0.2, 0.3, and 0.4 mL/min (with injections of 90 µL) were also tested. Eluent was monitored at 210 nm in all cases. Runs of GY(24) at 220 nm with 1.0 mL/min flow rate and 80 µL injections were performed, followed by GY(24) at 235 nm and 0.5 mL/min flow rate.

HFBA WITH PERKIN-ELMER SERIES 400 LIQUID CHROMATOGRAPH

Problems with stabilizing the baseline of the IBM LC became insurmountable, requiring up to 6 hours equilibration time. Thus, the Perkin-Elmer Series 400 HPLC from the Biology department was used to run samples. 50 μL of the following samples were prepared and run with 5 mM HFBA mobile phase at a flow rate of 1.0 mL/min while monitoring at 210 nm:

- 5 mM GY(std) in KPi buffer
- 5 mM Tyr in KPi buffer
- 5 mM Gly in KPi buffer
- 2.5 mM GY (24)

A UV spectrum was obtained for GYC from 200-320 nm. In prior experiments, no thought was given to the idea that catalase may produce some minor peaks. To investigate this possibility, HPLC was run on the following samples:

- 250 μL Fe(III)/200 μL H_2O_2/550 μL deionized water
- 250 μL Fe(III)/200 μL H_2O_2/50 μL catalase/500 μL deionized water
- 250 μL Fe(III)/200 μL H_2O_2/50 μL catalase/50 μL mannitol/450 μL deionized water
- 500 μL GY(24)/50 μL catalase/450 μL deionized water
- 500 μL GY(24)/50 μL catalase/50 μL mannitol /400 μL deionized water
- 500 μL GY(24)/50 μL catalase/250 μL mannitol/200 μL deionized water

Glycine consistently displayed two peaks, and a new bottle was used to rerun earlier HPLC trials to determine if any contaminant was present in the glycine obtained from Sigma.

50 μL samples of Gly-Tyr exposed to hydroxyl radical from 1 to 5 hours were prepared with 5 mM HFBA with a flow rate of 1.0 mL/min while monitoring at 210 nm.

Stage 4 Separation of GY(24) through Other Chromatographic Techniques

Materials: LK6D Silica Gel 60 Angstroms, from Whatman Inc., Clifton, NJ; glycine (Gly), tyrosine (Tyr), and glycyltyrosine (Gly-Tyr, GY) were purchased from Sigma Chemical Company, St. Louis, MO; hydrogen peroxide (H_2O_2), 1-butanol, chloroform, ammonium hydroxide, 1-propanol, acetic acid (HAc), ethyl acetate and diethyl ether were purchased from Fisher Scientific, Fairlawn, NJ; iron (III) sulfate [$Fe_2(SO_4)_3$] and methanol were purchased from J.T. Baker Chemical Company, Phillipsburg, NJ; and acetone was purchased from Aldrich Chemical Company, Milwaukee, WI. Instrumentation: injections for HPLC used a 100 μL syringe from Hamilton Company, Reno, Nevada; a polypropylene (10 cm x 10 mm) column with sinter disk was used for column chromatography; and lyophilization was performed on a Lyph-Lock 6 System by Labconco.

Other methods of separating the GY(24) components were investigated. First, several solvent systems were investigated to see if better separations of GY(24) were possible. Another attempt to separate the GY(24) involved freeze-drying, percolation column chromatography and flash chromatography.

OTHER SOLVENT SYSTEMS

Chromatography using Aluminum-backed silica chromatography plates were investigated using the following solvent systems: 70:30 (v/v) n-propanol:deionized water,

methanol, glacial acetic acid, ethyl acetate, diethyl ether, and 2:2:1(v/v/v) chloroform:methanol:17% NH_4OH.

LYOPHILIZATION

Lyophilization (freeze-drying) of GY(24) samples was performed in order to powder reaction products in preparation for column chromatography. The ice-collecting coil was lowered to -40 °C and the vacuum pump set at 100 microns. The temperature set point was set at -15 °C. Six 7 mL samples of the aqueous portion of GY(24) were frozen by using dry ice and acetone mixed in a dewar. Rotating the bottles quickly permitted the solution to freeze and coat the inner glass walls.

PERCOLATION COLUMN CHROMATOGRAPHY

Column Preparation

Once lyophilization of GY(24) samples was complete, a percolation column was prepared in an attempt to separate the components of these samples. Using the wet packing technique, a polypropylene column (10 cm x 10 mm) with sinter disk was prepared. The crude sample (25 mg) required 25-50 times the amount of silica gel adsorbant placed in the column. The column was packed with 1.25 grams of silica gel. The solvent was prepared using 2:2:1 (v/v/v) chloroform: methanol: 17% NH_4OH. The lyophilized sample (25 mg) was dissolved in 50 mL solvent and loaded onto the column. Fifty-five 10 mL fractions were collected over 8 hours.

TLC of Percolation Fractions

Using 70:30 (v/v) n-propanol:deionized water, a silica gel plate was spotted with fractions collected from percolation of GY(24), and with 5 mM Gly, 5 mM Tyr, and 2.5 mM GYC for comparison. Ninhydrin was used as the visualization reagent. Using 70:30 (v/v) n-propanol:deionized water on reversed-phase TLC plates, spotting of the first two of the fifty-five fractions was repeated.

CHAPTER 5

RESULTS AND DISCUSSION

Stage 1 Results: Initial Screening of Dipeptides

In pilot studies of various dipeptides in the presence of the hydroxyl radical, Gly-Gly, Gly-Glu, Gly-His, Gly-Met, Gly-Phe, Gly-Pro, Gly-Ser, Gly-Trp and Gly-Tyr were used as possible targets for cleavage sites. Peptide bonds absorb in the range of 210-220 nm. Thus, UV spectra of dipeptides before and after exposure to free radicals should reveal the presence or loss of this bond. Preliminary studies of UV spectra observed after 24 hours incubation showed significant spectral changes for Gly-His, Gly-Ser and Gly-Tyr over a range of 200-320 nm, while no change in the spectra occurred with the other dipeptides listed.

Only Gly-Tyr and Gly-His produced spots after TLC that did not correspond to the dipeptide itself. After 24 hours of exposure to free radicals, each of these dipeptides had one spot whose R_f value corresponded to Gly. Gly-Tyr had one other spot and Gly-His had three other spots whose R_f values did not correspond to either amino acid standard or to the dipeptide itself. Controls using dipeptide with H_2O_2 alone or metal ion alone resulted in no changes after TLC. To determine if the order of the amino acid made a difference to site selection, Ala-Tyr, Pro-Tyr and Tyr-Gly were used as possible reaction targets with the hydroxyl radical. UV results showed a change in the spectra from 200-225 nm for all three, although the change seen for Pro-Tyr was not as dramatic.

TLC using 70:30 (v/v) n-propanol:water indicated two spots for Ala-Tyr and Tyr-Gly, one near each of their standards, while Pro-Tyr had one spot, near its standard. Ala-Tyr and Ala-Tyr(std) both had a spot corresponding to Tyr, which indicates partial hydrolysis of the dipeptide standard.

GLY-HIS

The ultraviolet spectra of Gly-His(std) showed a peak absorbance between 210-230 nm while Gly-His exposed to free radicals for 24 hours at 37°C showed a steady decrease in absorbance with time throughout this range (Figure 3).

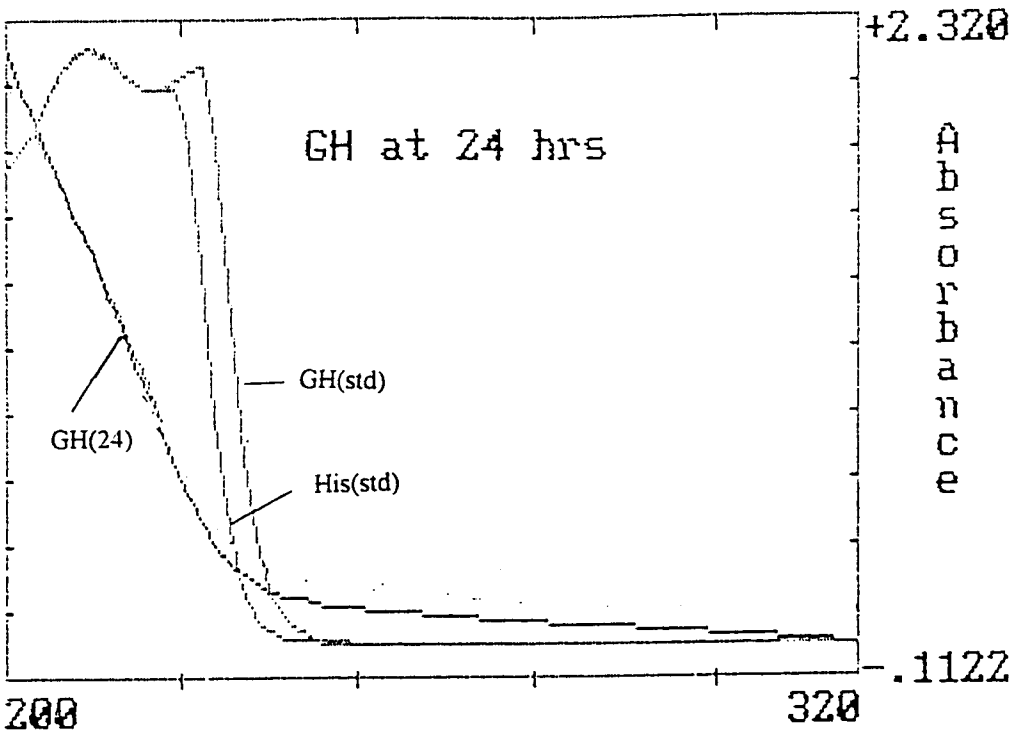

Figure 3 UV Spectra of Gly-His and Standards

TLC of Gly-His samples [3:1:1(v/v/v)1-butanol:HAc:deionized water] revealed no change in spotting for the dipeptide incubated with Fe(III) or H_2O_2 alone when compared to the standard dipeptide. However, a spot with an R_f value similar to Gly appeared for the dipeptide incubated with Fe(III) and H_2O_2 together for 24 hours, one spot corresponding to the Gly-His standard and two spots which do not correspond to the standards (Table 1). One less spot occurred with the sample incubated for 19 hours.

TABLE 1 TLC OF GLY-HIS (butanol/HAc solvent)

Sample	*Rf*	*Spotting*
Gly	0.234	large purple spot
His	0.107	small purple spot
GH(std)	0.073	purple band
GHC	0.074	purple band
GHFe	0.075	purple band
GHP	0.079	purple band
*GH(19)	0.079, 0.212, 0.246	pink spots
*GH(24)	0.078, 0.181, 0.207, 0.252	pink spots

*GH(19) and GH(24) represents dipeptide exposed to free radical for 19 and 24 hrs, respectively.

In an attempt to improve the separation, solvent was prepared using 15:3:10:12(v/v/v/v)1-butanol:HAc:pyridine:deionized water. GH(24) produced only one spot with an R_f value different than the standard dipeptide or the individual amino acids (Table 2). The pyridine solvent was not as effective as the 1-butanol/HAc solution in separating the components of GH(24).

TABLE 2 TLC OF GLY-HIS (pyridine solvent)

Sample	*Rf*	*Spotting*
Gly	0.446	large pink spot
GH(std)	0.315	small salmon spot
His	0.426	pale lavender spot
GH(24)	0.389	small salmon spot

GLY-MET

The TLC of Gly-Met samples developed in 70:30(v/v)1-propanol:deionized water revealed the results listed in Table 3. The Gly-Met standard produced two spots, one possibly caused by the presence of oxidized Met in the standard. Gly-Met with Fe(III) alone did not lose the primary spot corresponding to the dipeptide control. However, Gly-Met with H_2O_2 alone and GM(24) each had a large spot with a much smaller R_f value than the dipeptide control. The results with hydrogen peroxide were confusing, and may have indicated metal ion contamination.

TABLE 3 TLC OF GLY-MET

Sample	*Rf*	*Spotting*
Gly	0.28	purple spot
Met	0.516, 0.240	purple spot, faint spot
GM(std)	0.329, 0.140	purple spot, faint spot
GMC	0.4, 0.146	purple spot, faint spot
*GMFe	0.396	large purple spot
*GMP	0.155	large purple spot
GM(24)	0.148	large purple spot

* GMFe - dipeptide with metal ion only; GMP- dipeptide with peroxide only

In order to investigate possible contamination by metal ion, the GMP sample (made with 5 mM EDTA/KPi buffer) was incubated at 37 °C and TLC was repeated. Again, there was still a change from the dipeptide control (Table 4).

TABLE 4 TLC OF GLY-MET (WITH EDTA)

Sample	*Rf*	*Spotting*
GM(std)	0.5	purple spot
GMP	0.408	purple spot
GMC	0.504	purple spot
Gly	0.378	purple spot
Met	0.63	purple spot

UV spectroscopy of GM(std) and GM(24) both showed a peak absorbance at 200-220 nm with no significant difference (Figure 4). After buffering Gly-Met with EDTA to prevent metal interaction with H_2O_2, no significant difference was found in the UV spectra of GM(std) and GMP.

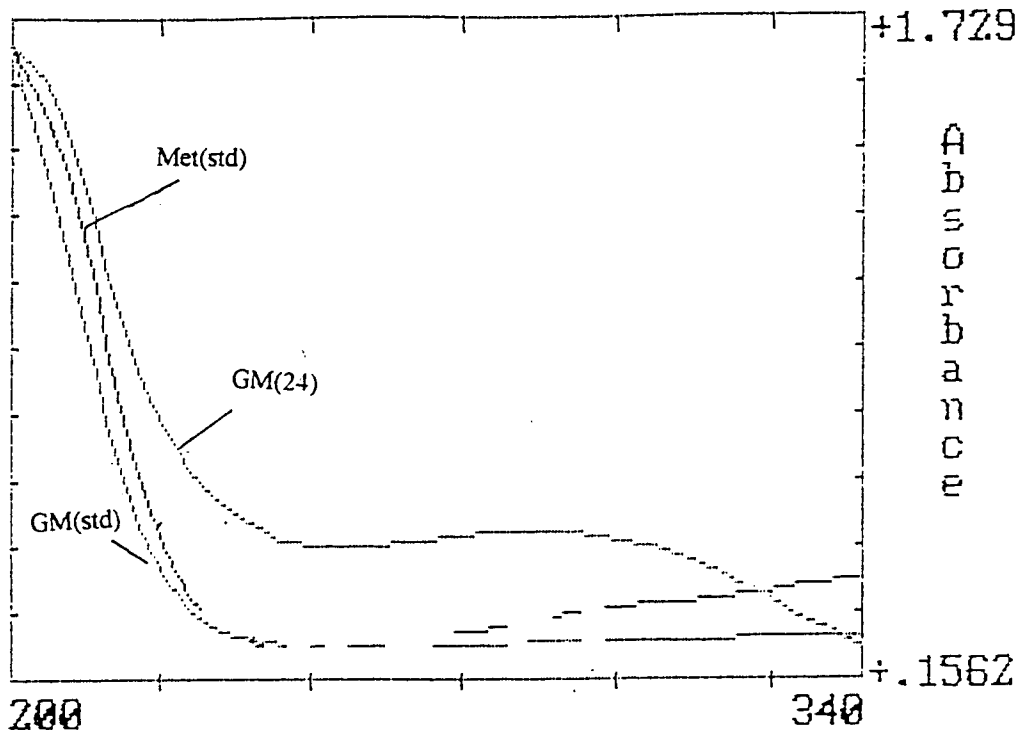

Figure 4 UV Spectra of Gly-Met and Standards

GLY-TYR

The TLC of Gly-Tyr showed no change in spotting when Gly-Tyr was exposed to H_2O_2 or Fe(III) alone (Table 5). In the presence of both, the spot corresponding to Gly-Tyr disappears after 24 hours, while two new spots, one with an R_f value corresponding to Gly appeared.

TABLE 5 TLC OF GLY-TYR

Sample	*Rf*	*Spotting*
Gly	0.236	purple spot
Tyr	0.479	lavender spot
GYC	0.384	lavender spot
GYFe	0.378	lavender spot
GYP	0.38	lavender spot
GY(24)	0.229, 0.164	faint violet spots

GY incubated with free radical from 1 - 9 hours produced spots with R_f values similar to GYC.

The UV spectrum of GY(std) showed a peak absorbance at 225 nm, whereas GY(24) showed a significant decrease at this absorbance (Figure 5), indicating a possible change in the dipeptide bond.

An ammonia assay was used to investigate the deamination of the α-amino group. Samples prepared for testing were mixed with GLDH solution and equilibrated for 10 minutes. Relatively little change occurred with the Gly-Tyr control at 0 minutes, whereas samples incubated with Fe(III) and H_2O_2 showed a progressive increase in NH_3 production over time (Table 6).

TABLE 6 AMMONIA ASSAY OF GLY-TYR

Sample	**Ammonia (micrograms/ml)*
Control	6.96
GY(0)	-0.15
GY(3)	0
GY(6)	0.2065
GY(24)	6.83

*Absorbance at 340 nm

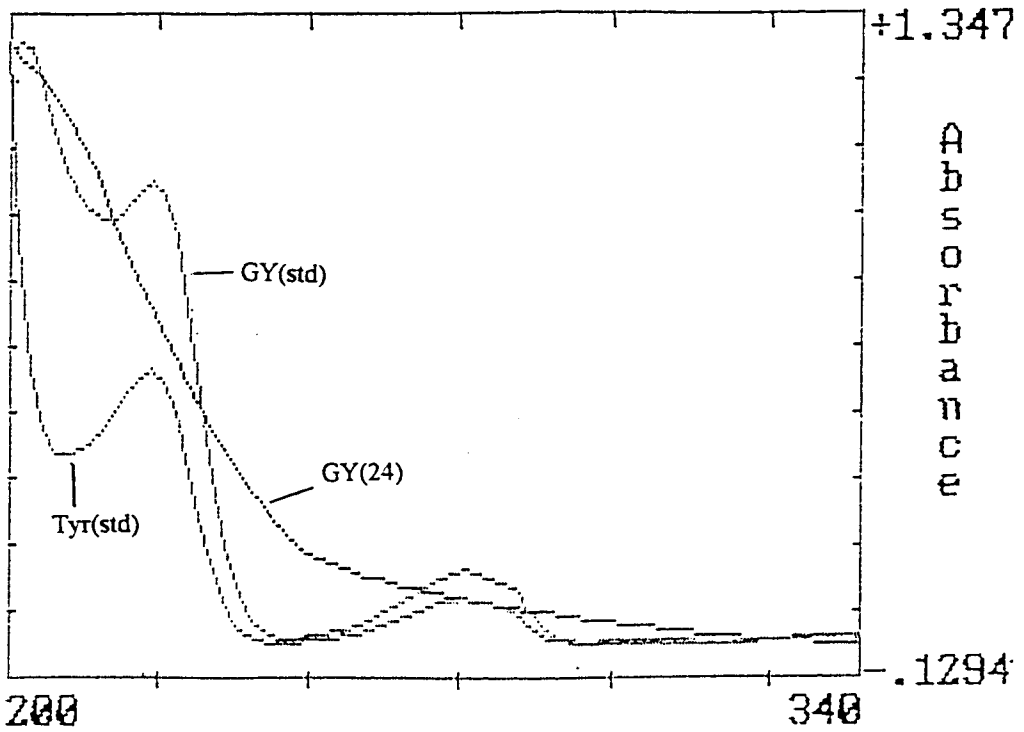

Figure 5 UV Spectra of Gly-Tyr and Standards

There was no linear relationship between the amount of NH_3 produced and the amount of time the Gly-Tyr was incubated with hydroxyl radical. The instructions for the diagnostic kit stated the control should produce 5 μg/ml of NH_3. The control in this study exhibited a 39% error. In addition, the test kit mentioned Fe(III) was an inhibitor of the GLDH enzyme. The assay was performed again in the presence of EDTA to chelate Fe(III). The results are given in Table 7.

TABLE 7 PRODUCTION OF AMMONIA (micrograms/ml)

Sample	*Initial*	*3 hours*	*6 hours*	*11 hours*
GYC	-0.753	0.265	0.752	-0.003
GY	2.91	2.54	0.177	1.1
GHC	0.756	-0.537	0.0885	-0.297
GH	-0.19	3.24	3.48	5.08

Although there was an increase in the production of NH_3 over time with Gly-His, the results for Gly-Tyr were inconclusive since there was some fluctuation with NH_3 production over time.

An attempt to acetylate Gly-Tyr was carried out to block possible metal chelation sites, thereby preventing its metal catalyzed oxidation (*40*). Variations in experimental conditions such as pH and acetic anhydride concentration were factors that determined whether acetylation occurred at the N-terminus or the hydroxyl group of tyrosine. At pH 9, both sites are targets. However, the experiment was performed at pH 7.48 which favors acetylation of the phenolic hydroxyl group. The structure of the desired product is given in Figure 6 (*39*).

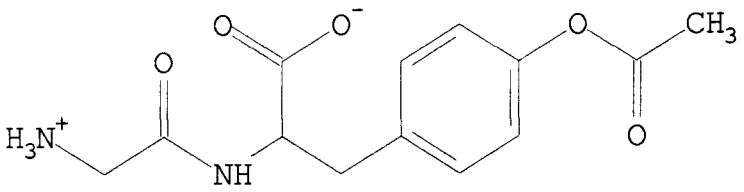

Figure 6 Acetylated Gly-Tyr

TLC was performed on Gly-Tyr and samples monitored over 90 minutes to determine if the structure had been acetylated (Table 8). There was an immediate change in the acetylated sample, which showed no spotting throughout the 90 minutes, indicating the Gly-Tyr had been altered or too dilute for TLC analysis.

TABLE 8 TLC OF GLY-TYR WITH ACETIC ANHYDRIDE

Sample	*Rf at 0 min*	*Rf at 30 min*	*Rf at 60 min*	*Rf at 90 min*
GY	0.739	0.645	0.655	0.58
GY(acet.anhyd)	—	—	—	—

UV spectra of Gly-Tyr and acetylated Gly-Tyr (Figure 7) revealed a shift in the peak absorbance (Gly-Tyr at 290 nm, acetylated Gly-Tyr at 280 nm). The literature (*39*) predicted a shift at 275 nm.

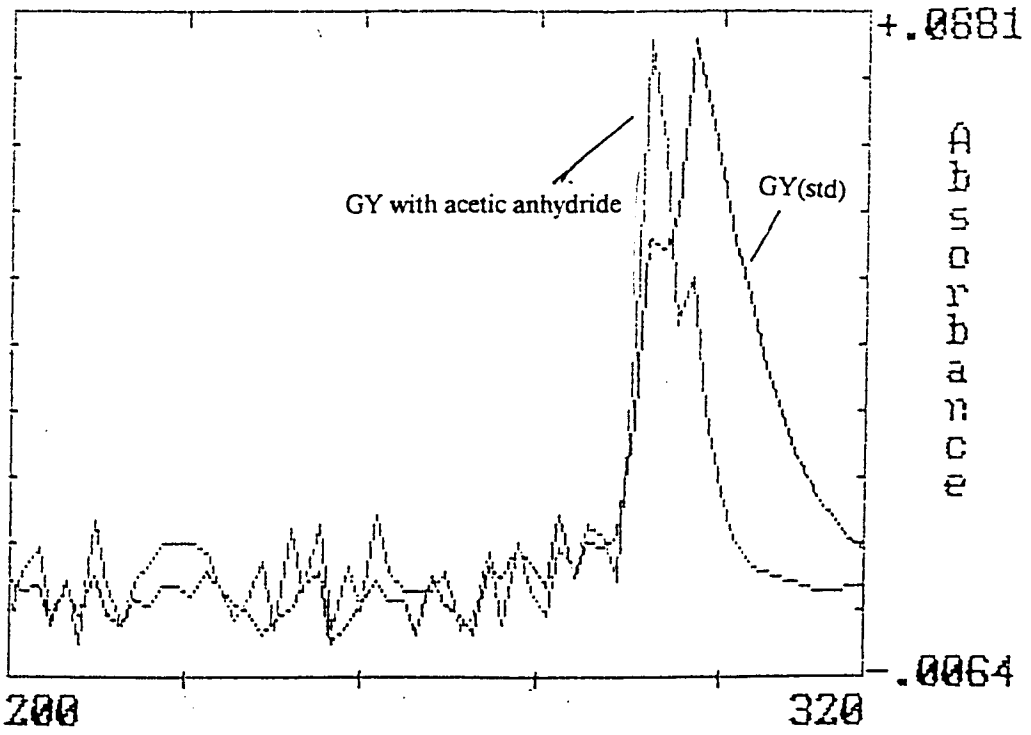

Figure 7 UV Spectra of Gly-Tyr before and after Acetylation

Difference spectra between Gly-Tyr and the possibly acetylated Gly-Tyr were obtained over one hour during the course of the reaction between 274-284 nm. The results are summarized in Table 9.

TABLE 9 CHANGE IN ABSORBANCE GLY-TYR vs. ACET. GLY-TYR

Time	*274 nm*	*276 nm*	*278 nm*	*280 nm*	*282 nm*	*284 nm*
5 min	0.0267	0.0291	0.0592	0.0451	0.0479	0.0734
10 min	0.0318	0.0328	0.0627	0.0442	0.0498	0.0725
15 min	0.0381	0.0282	0.0592	0.0502	0.0588	0.0667
20 min	0.0339	0.033	0.0599	0.0448	0.0565	0.0689
25 min	0.0384	0.033	0.0549	0.041	0.0603	0.0692
30 min	0.0362	0.0312	0.0567	0.0417	0.0501	0.0635
35 min	0.0363	0.0371	0.058	0.0476	0.0558	0..0734
40 min	0.0306	0.0328	0.0595	0.0464	0.0533	0.0622
45 min	0.0524	0.039	0.0671	0.0631	0.055	0.0815
60 min	0.0452	0.034	0.0521	0.0467	0.0482	0.0686

The maximum increases in absorbances occurred after 45 minutes for nearly all wavelengths. To obtain percentage acetylation, absorption data were averaged over the range 274-276 nm (since the literature specifies 275 nm as the predicted shift) and calculated as follows:

% Acetylation = ([Gly-Tyr] with acetic anhydride / initial [Gly-Tyr]) x 100

[Gly-Tyr] with acetic anhydride = Δ absorbance / $\Delta\varepsilon_m$ x 1 cm

$\Delta\varepsilon_m$ = 1280 at 275 nm

Δ absorbance = Abs (Gly-Tyr with acetic anhydride) - Abs (initial)

Inital [Gly-Tyr] = 0.0833 M

Results of these calculations indicated a maximum percentage of acetylation after 45 minutes of 0.0429%.

TLC of the acetylated sample in sodium acetate buffer (using a 530-fold excess acetic anhydride) produced a spot with a R_f value of 0.600, which was different than the

GY(std) of 0.677. UV spectra on the sample with a 530-fold excess acetic anhydride indicated a 0.227% acetylation. The only way to increase the percentage yield was to use a much greater amount of acetic anhydride. Unfortunately, the accompanying decrease in the concentration of Gly-Tyr made it too dilute and the signal/noise became too large to detect Gly-Tyr. TLC of the acetylated (530-fold excess) Gly-Tyr exposed to the hydroxyl radical and incubated for 24 hours was inconclusive, as no spotting occurred with the controls or the acetylated Gly-Tyr.

UV spectra of the acetylated Gly-Tyr (2000-fold excess) exposed to hydroxyl radical displayed a peak absorbance at 295 nm. The acetylated sample's absorbance was less intense than the GY(24), but greater than the acetylated control (not exposed to hydroxyl radical).

Acetylation of the phenolic hydroxyl of Tyr can be reversibly deacetylated with hydroxylamine (*40*). If acetylation of Gly-Tyr occurred only at the phenolic hydroxyl group, addition of hydroxylamine should remove the acetyl group and produce the unmodified dipeptide. Attempts to reverse the acetylation of Gly-Tyr, TLC revealed no spotting of AGY with the addition of 10 mM and 100 mM hydroxlyamine.

Carbobenzoxy chloride was used to block the N-terminus of Gly-Tyr. TLC of CBZ-Gly-Tyr revealed a new spot with a substantially higher R_f value (0.823) than the Gly-Tyr standard (0.589) when developed with ninhydrin. A new spot with a lower R_f value than the Gly-Tyr standard (0.616 vs. 0.708) appeared upon treatment with Pauly Reagent, which is specific for tyrosine and histidine residues.

In an attempt to reduce random oxidation and investigate site-specificity, Gly-Tyr samples were incubated with mannitol, a free radical scavenger. TLC indicated no significant changes in the R_f values between the dipeptide control and the samples containing mannitol (Table 10).

TABLE 10 TLC OF GY(24) WITH MANNITOL

Sample	*Rf*	*Spotting*
GY(std)	0.664	yellow
GYC	0.668	yellow
G	0.487	peach
Y	0.755	lavender
GYM	0.681	pale yellow
GY(24)	0.805	pale spot
GYM(24)	0.682	pale yellow
GY(100 P)	---	---
GYM(100 P)	0.682	pale yellow
GY(50 P)	---	---
GYM(50 P)	0.693	pale yellow
GY(150 Fe)	---	---
GYM(150 Fe)	0.694	pale yellow
GY(100 Fe)	0.695	pale yellow
GYM(100 Fe)	0.706	pale yellow

* All GY samples contain 500 μL GY and enough deionized water to bring the total volume to 1.0 ml. The contents of the remaining samples are: GYM - 250 μL mannitol; GY(24) - 200 μL Fe, 250 μL H_2O_2; GYM(24) - 200 μL Fe, 150 μL H_2O_2, 150 μL mannitol; GY(100 P) - 200 μL Fe, 100 μL H_2O_2; GYM(100 P) - 200 μL Fe, 100 μL H_2O_2, 100 μL mannitol; GY(50 P) - 200 μL Fe, 50 μL H_2O_2; GYM(50 P) - 200 μL Fe, 50 μL H_2O_2, 50 μL mannitol; GY(150 Fe) - 150 μL Fe, 150 μL H_2O_2; GYM(150 Fe) - 150 μL Fe, 150 μL H_2O_2, 150 μL mannitol; GY(100 Fe) - 100 μL Fe, 100 μL H_2O_2; GYM(100 Fe) - 100 μL Fe, 100 μL H_2O_2, 100 μL mannitol.

The UV spectra of GY(24) with mannitol indicated that GY(100P) and GY(150 Fe) had a loss of peak absorbance at 225 nm. Gly-Tyr treated with mannitol had the same spectrum as GY(std), and did not show the dramatic change which occurred with untreated GY(24) (Figure 8). GY(100Fe) and GY(50P) had peak absorbances at 205 nm, and GY(50Fe) had maxima at both 205 and 225 nm.

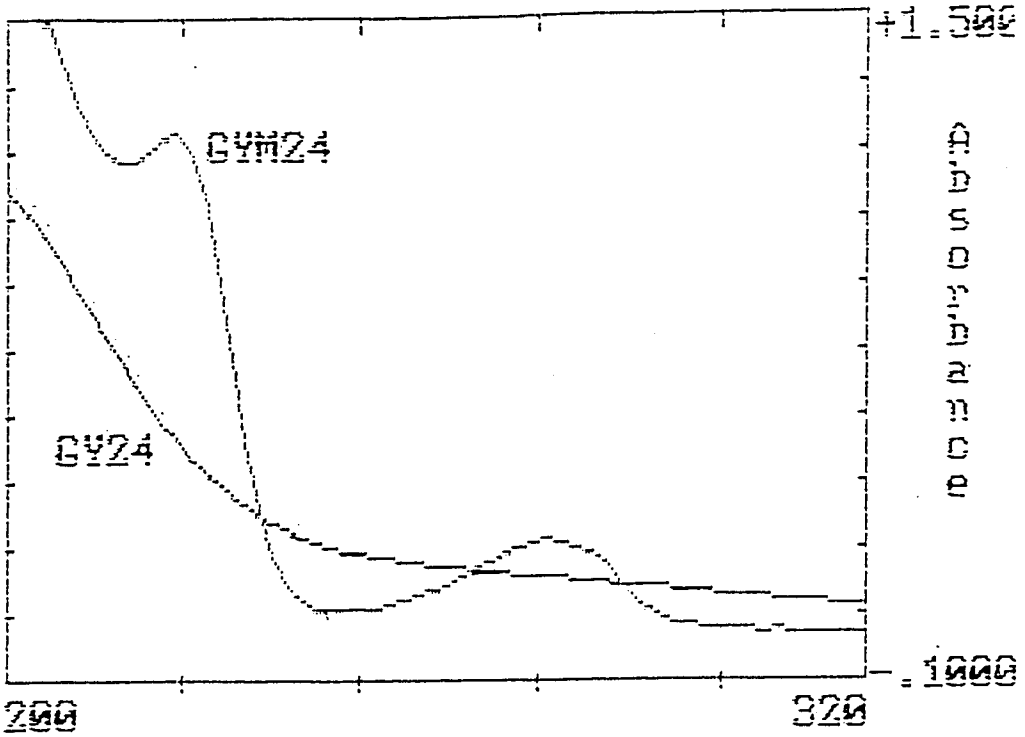

Figure 8 UV Spectra of Gly-Tyr exposed to free radical for 24 hours with and without mannitol.

Stage 2 Results: Various Metal Ions

Results of TLC on Gly-Tyr, Ala-Tyr, and Pro-Tyr in the presence of copper(II) and H_2O_2 are summarized in Table 11. GY(24) had two spots, one near Gly and one different than either amino acid or dipeptide control. AY(24) had two spots, one near Ala and one different than the controls. PY(24) had no spots. None of the dipeptides showed changes in the presence of metal ion or H_2O_2 alone.

TABLE 11 TLC OF GY, AY, PY WITH COPPER(II)

Sample	*Rf*	*Spotting*
Gly	0.344	lavender
Tyr	0.667	lavender
GY(std)	0.534	marigold
GYC	0.538	marigold
GYCu	0.542	marigold
GYP	0.543	marigold
GY(24)	0.337, 0.460	pale pink
Ala	0.421	purple
AY(std)	0.583	purple
AYC	0.578	purple
AYCu	0.576	purple
AYP	0.574	purple
AY(24)	0.4, 0.481	light purple, narrow band
Pro	0.346	pale yellow
PY(std)	0.423	peach
PYC	0.418	peach
PYCu	0.415	peach
PYP	0.415	peach
PY(24)	---	---

UV spectra of GY(24) (Figure 9), AY(24) (Figure 10) and PY(24) (Figure 11) using Cu(II) indicated that they all lost peak absorbances between 200 - 240 nm, whereas Cu(II) and H_2O_2 controls matched the spectra of their respective standards.

To determine if free radicals existed after the reaction had been stopped with catalase, timed treatment with murexide was investigated. Murexide has a peak absorbance of 520 nm. In the presence of free radicals murexide is bleached. The loss of absorbance at 520 nm indicates free radicals are present. GY(24), AY(24) and PY(24) were examined in the presence of murexide. Spectra from 430-630 nm were obtained at 0, 5 and 10 minutes. No bleaching occurred for GY(24) and PY(24), but AY(24) showed a shift in the maximum wavelength.

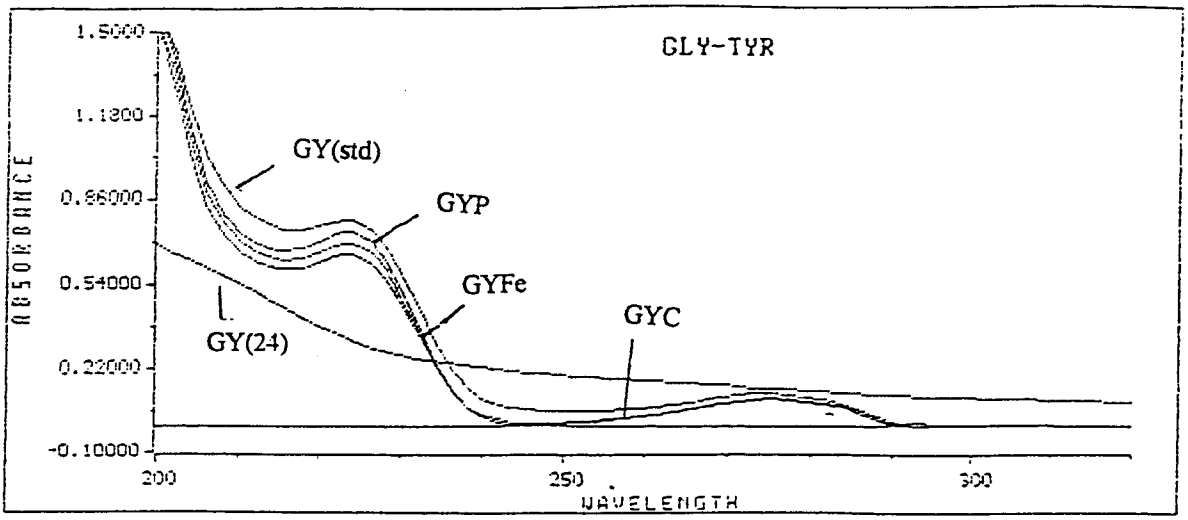

Figure 9 UV Spectra of Gly-Tyr before and after exposure to Cu(II) and H_2O_2

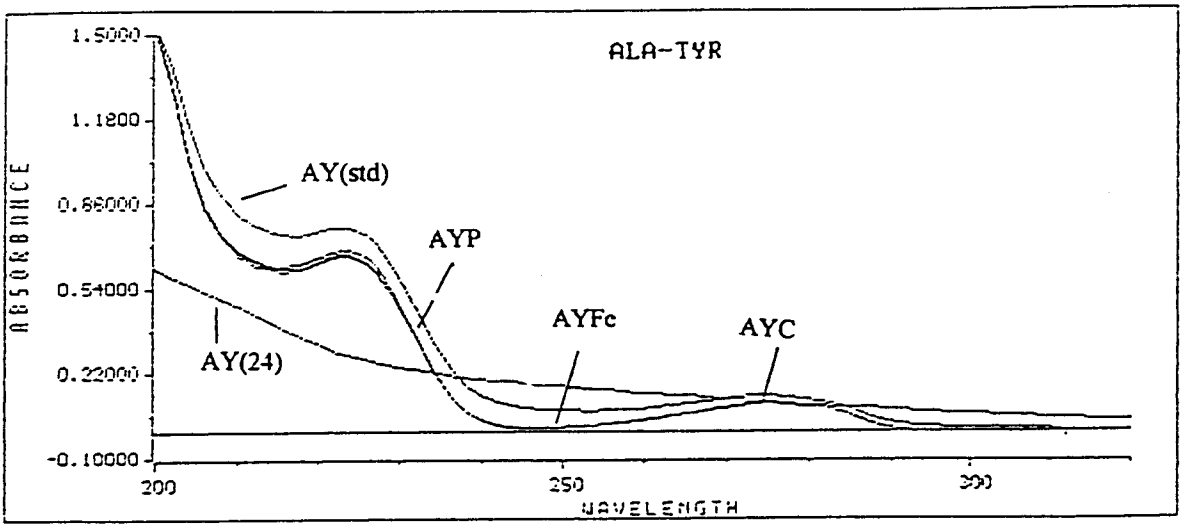

Figure 10 UV Spectra of Ala-Tyr before and after exposure to Cu(II) and H_2O_2

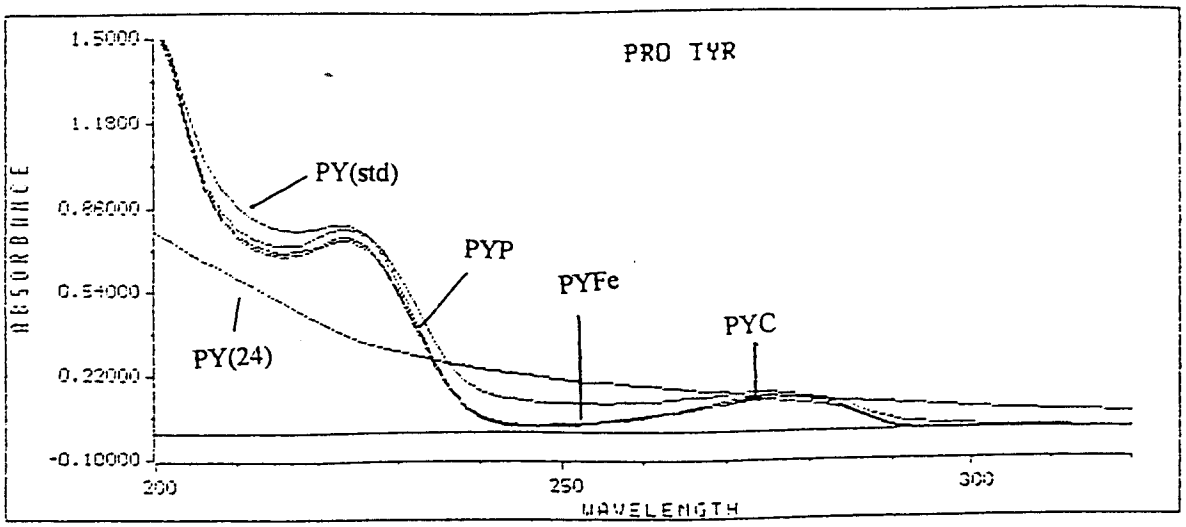

Figure 11 UV Spectra of Pro-Tyr before and after exposure to Cu(II) and H_2O_2

The addition of 50 μL of n-butanol to 3 mL of these samples inhibited the bleaching of murexide. Vitamin C was also used as a deterrent to free radical formation. The Vitamin C did not fully protect the dipeptide as the Gly spot still occurred with the TLC test of GY(24). A second antioxidant, butylated hydroxytoluene (BHT) in methanol added to AY(24) showed no decrease in murexide absorbance at 520 nm. In addition, AY(24) was tested with urea, thiourea and mannitol. Only the mannitol sample still had any absorbance at 520 nm.

Upon TLC analysis, the dipeptide spots disappeared with GY-Cu and GY-Co after 24 hours of incubation. One spot occurred with GY-Ni, whose R_f value was intermediate between GYC and the Tyr standard. AY-Ni and AY-Co both had one spot with R_f values lower than the dipeptide or Tyr standard, but higher than Ala standard. No spots appeared with AY-Cu after 24 hours of exposure.

TLC experiments of Gly-Tyr with Fe(II) and H_2O_2 had a loss of the spot corresponding to the dipeptide control. Uv spectra indicated GY(24) with Fe(II) behaved similarly as GY(24) with Fe(III).

Stage 3 Results: Analysis of Reaction Products by HPLC

HEPTANESULFONATE AS MOBILE PHASE

A variety of sample size injections and flow rates were attempted to select the best separation conditions. Broad peaks with no return to the baseline occurred with flow rates of 1.0 and 2.0 mL/min using 100 μL injections of 5 mM Gly(std) and 5 mM Gly at room temperature. A flow rate of 2.0 mL/min created very high pressure and caused a leak in the system which could not be fixed at that flow rate. Broad peaks occurred with 100 μL injections of 2.5 mM Tyr when run at a flow rate of 1.2 mL/min at 30 °C.

Using 20 μL injections of 0.5 mM concentrations and a flow rate of 1.2 mL/min at 30 °C, Gly had two peaks (Figure 12), at 6.849 and 13.904 min. Tyr had one peak (Figure 13) at 11.7 min, and GY(std) had two peaks (Figure 14) at 4.7 and 11.7 min.

In order to obtain enough sample passing through the HPLC for use in UV analysis, multiples of each standard were collected after injecting 40 μL of 0.5 mM samples (20 nmol of sample). GYC had two peaks (Figure 15), at 4.876 and 11.912 min. GY(24) had five peaks (Figure 16) at 1.719, 3.322, 6.378, 12.475, and 17.462 min. No results were obtained with the TLC of Gly, Tyr, GYC and GY(24) eluents first run through the HPLC. Although the 20 nmol injections produce good HPLC peaks, the samples retrieved were too dilute for TLC detection and ultimate verification.

UV spectra showed a weak signal for Tyr when using a minimum of 125 nmol sample. To obtain 125 nmol Tyr for UV detection, an injection of 50 μL of 2.5 mM Tyr

was required. However, injection of this much sample for HPLC analysis overloaded the system. Using the HPLC eluent from a 40 μL injection of 0.5 mM GYC (20 nmol), the 4.076 minute sample matched the absorbance at 220 nm of the GY(std), while the 11.912 minute peak had no absorbance from 220-340 nm.

Negative peaks in the chromatograms were described by Levin and Grushka (*41*) as "system peaks." Peak A was due to the presence of the Na^+ ion. Peak C was due to Cu(II) while Peak D was due to the sulfonate ions. Peak B (acetate) was the only positive peak. Of primary concern was the possibility of masking a reaction product's peak by simultaneous elution of a system peak. Peak A eluted before all solutes and could be treated as the void volume indicator. Peak B eluted before the polar molecules. Both peaks were fairly constant over a variety of experimental conditions and did not interfere greatly with amino acid analysis. Peaks C and D were intensely negative and might have masked nearby solute peaks. In order to counteract Peak C, the concentration of Cu(II) in the mobile phase needed to approximate the concentration of the dipeptide in the injection sample. To overcome the predominance of Peak D, the injected sample needed to contain the same concentration of sulfonate as present in the mobile phase.

To reduce or eliminate system peaks, standards were first diluted with Cu(II)/heptanesulfonate buffer. Using 40 μL of 0.5 mM Gly(std), one major peak at 6.799 minutes was obtained. When Tyr was used instead, there was no sign of the Tyr peak. In earlier trials, Tyr had a peak at 11.7 minutes. To determine if the earlier trials displayed a system peak, Tyr was rerun for 30 minutes and 60 minutes at 30 °C, for 60 minutes at 34 °C, and 60 minutes at 40 °C. A peak was obtained with the last trial after 35.0 minutes.

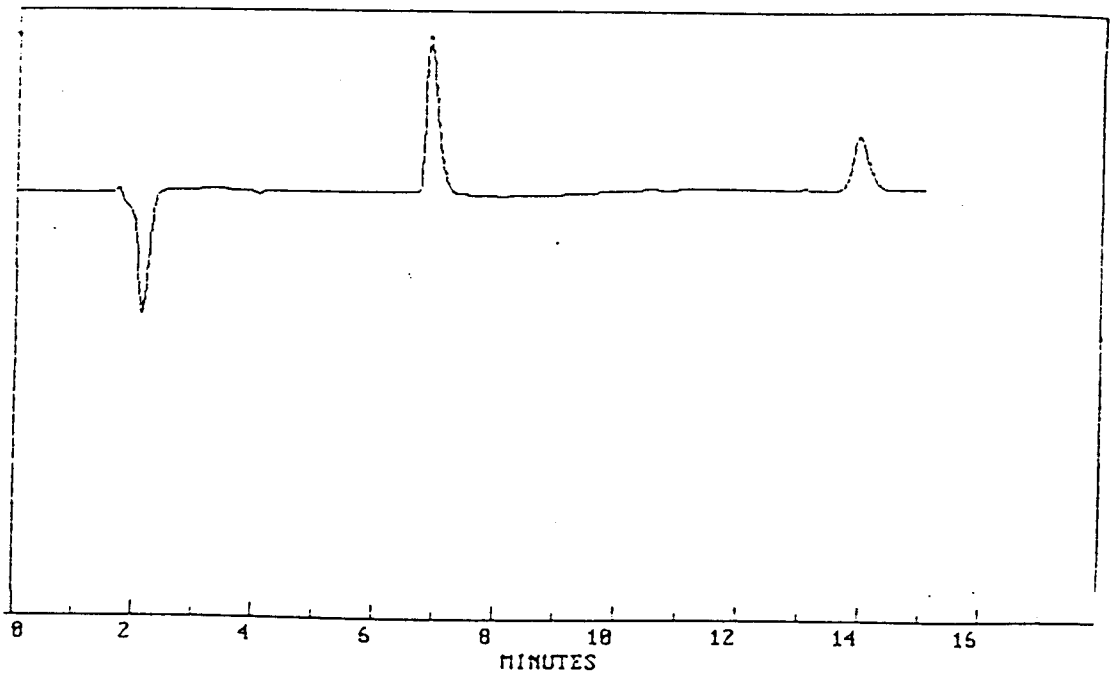

Figure 12 HPLC of 0.5 mM Gly (heptanesulfonate mobile phase, 30°C, flow rate of 1.2 mL/min, 210 nm)

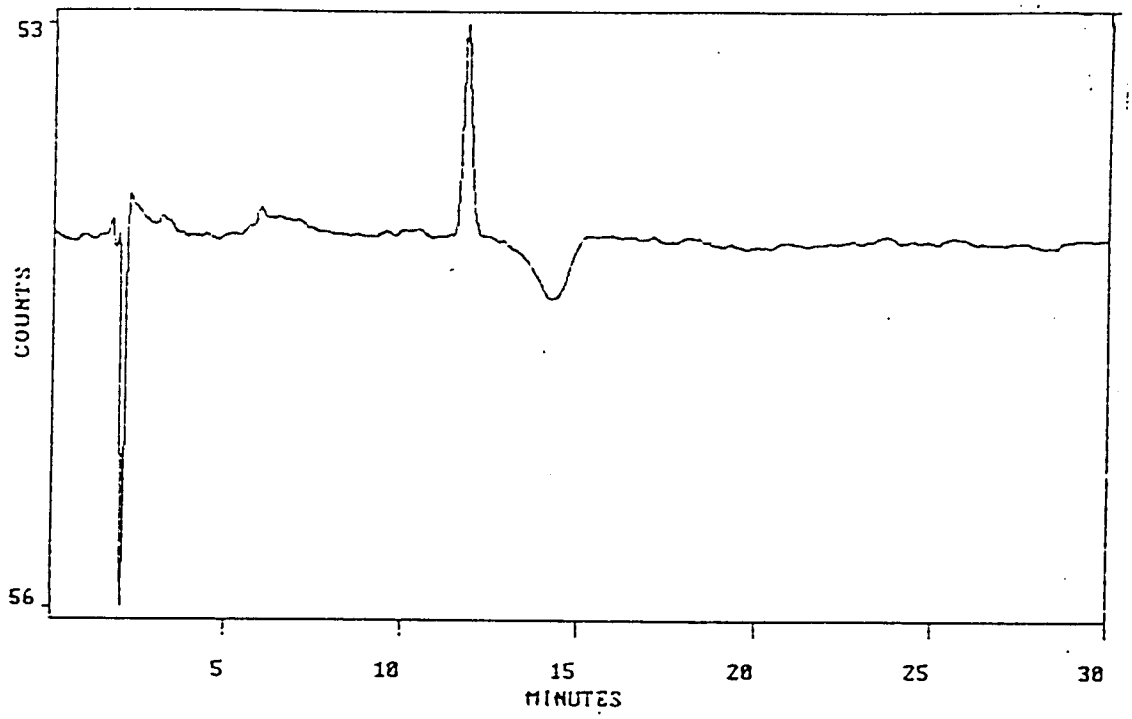

Figure 13 HPLC of 0.5 mM Tyr (heptanesulfonate mobile phase, 30°C, flow rate of 1.2 mL/min, 210 nm)

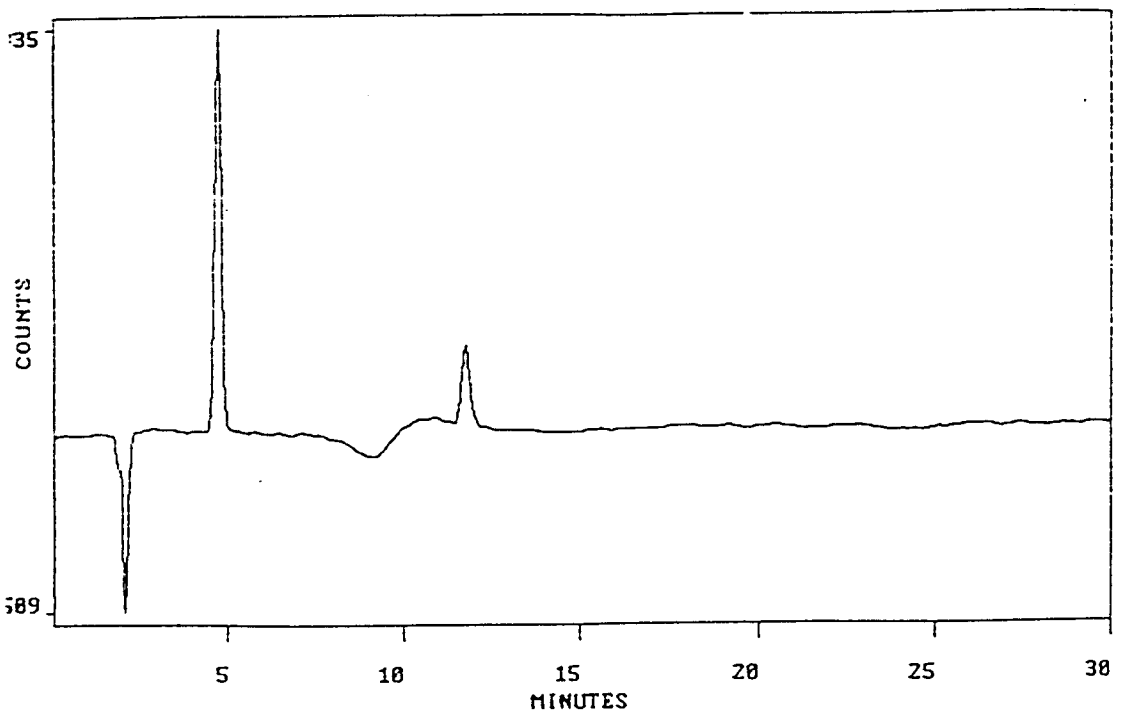

Figure 14 HPLC of 0.25 mM Gly-Tyr standard (heptanesulfonate mobile phase, 30°C, flowrate of 1.2 mL/min, 210 nm)

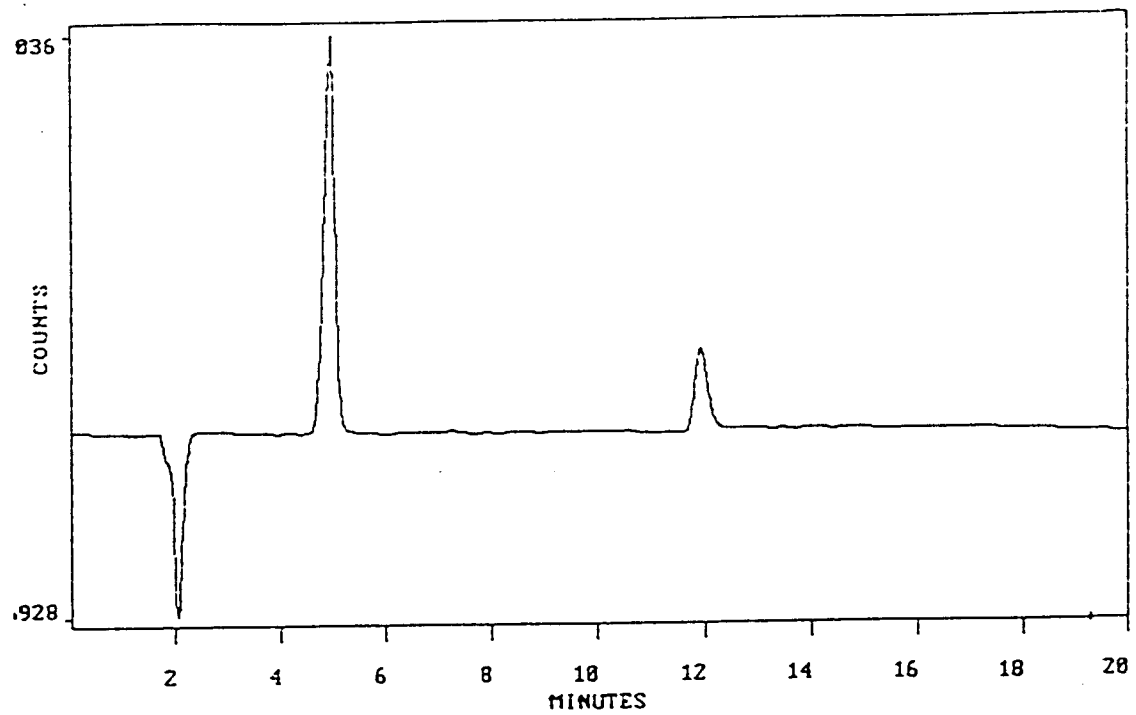

Figure 15 HPLC of 20 nmol GYC (heptanesulfonate mobile phase, 30°C, flow rate of 1.2 mL/min, 210 nm)

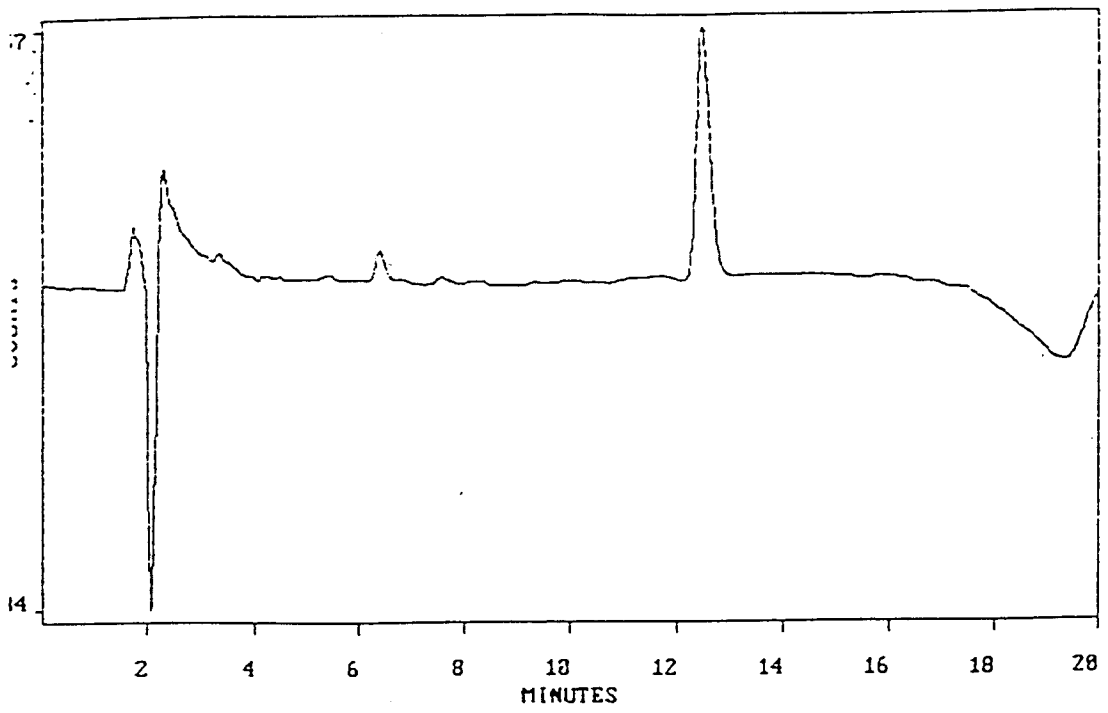

Figure 16 HPLC of 0.5 mM GY(24) (heptanesulfonate mobile phase, 30°C, flow rate of 1.2 mL/min, 210 nm)

At higher temperatures, the literature stated there would be a decrease in the retention times, but with an accompanying decrease in the stability of the baseline. In order to reduce retention times, the following parameters were used: 0.8 mM heptanesulfonate buffer, at 40°C, and 40 µL injections of 0.5 mM samples (standards were 5 mM prior to dilution with the heptanesulfonate buffer). Under these conditions, Gly had one peak at 2.915 min, Tyr one peak at 26.29 min, GYC one at 3.292 min and GY(24) had five peaks at 1.919, 2.959, 5.75, 6.426 and 7.3 min (Figure 17). The system peaks had been substantially reduced.

Experiments to resolve the early peaks of GY(24) used 0.8 mM heptanesulfonate buffer at 30 °C and produced five peaks with similar retention times as in the preceeding paragraph. To further resolve the peaks, the concentration of heptanesulfonate was

increased to 2.5 mM and the temperature was increased to 40 °C. A major peak at 2.152 min and minor peaks at 1.762, 1.924, 4.883 and 11.175 min resulted using these conditions.

The concentration of heptanesulfonate was then increased to 5 mM with a corresponding decrease in temperature to 30 °C. A major peak at 2.229 min and minor peaks at 2.556, 6.541, and 12.925 minutes were generated. The increase in the heptanesulfonate concentration spread out the peaks, although not substantially.

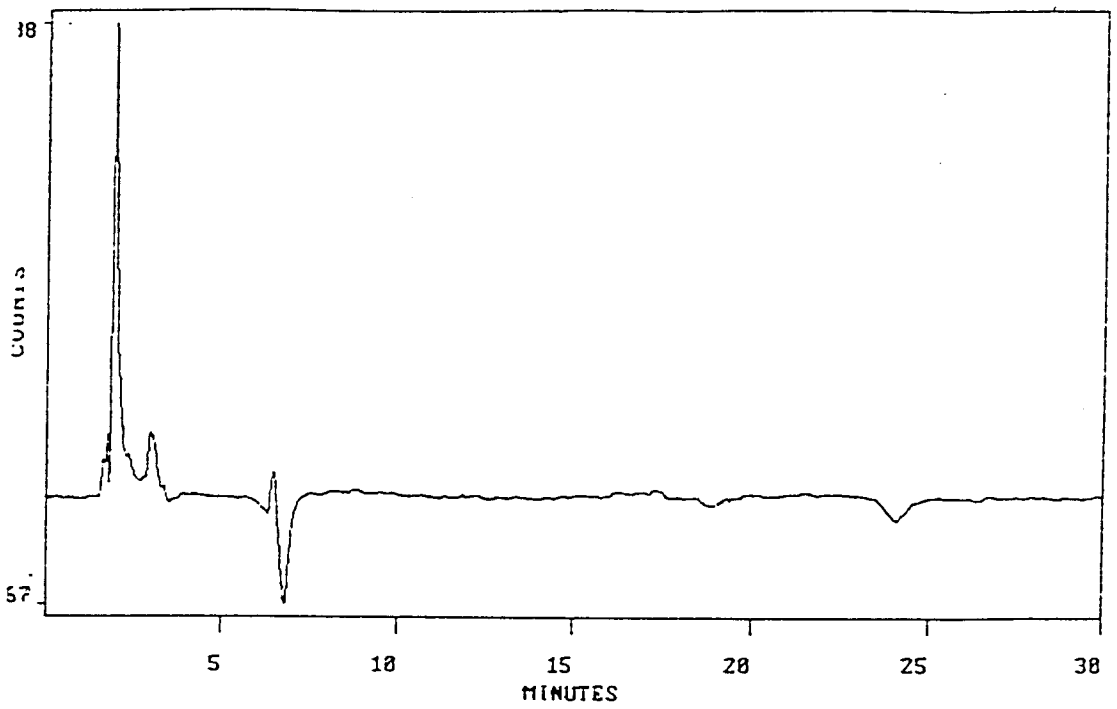

Figure 17 HPLC of 0.5 mM Gly-Tyr diluted in mobile phase (0.8 mM heptanesulfonate, 40°C, flow rate of 1.2 mL/min, 210 nm)

UV detection of murexide from 430-630 nm showed no decrease in absorbance of GY(24) with methanol (Figure 18), but there was a steady decrease in absorbance in the

sample without methanol when measured after 5 and then 10 minutes (Figure 19). Thus, methanol was able to quench any trace of free radicals still in solution.

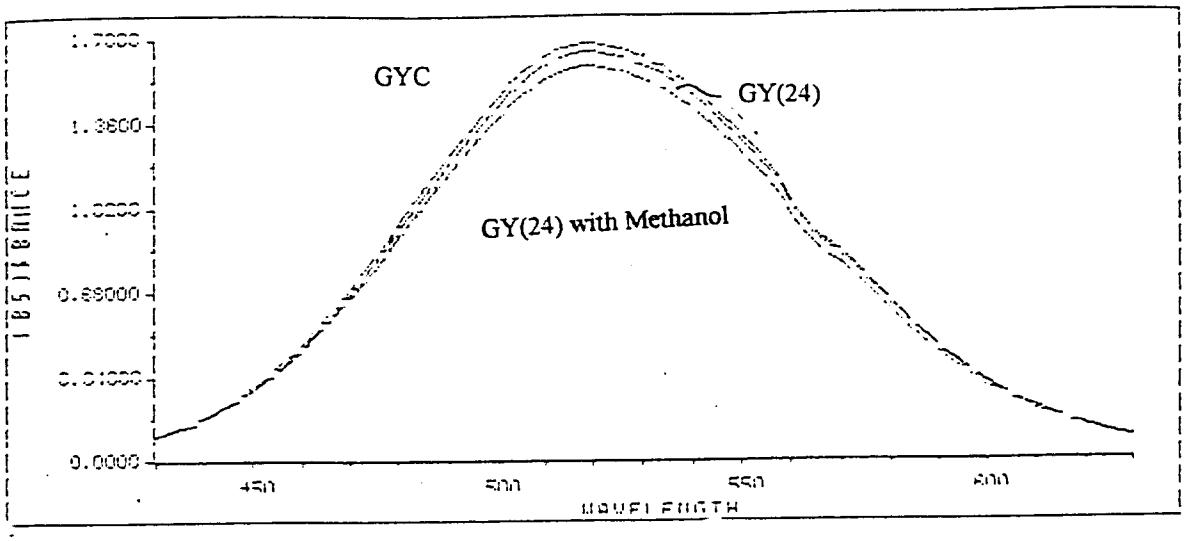

Figure 18 UV Spectra of GYC, GY(24) and GY(24) with Methanol

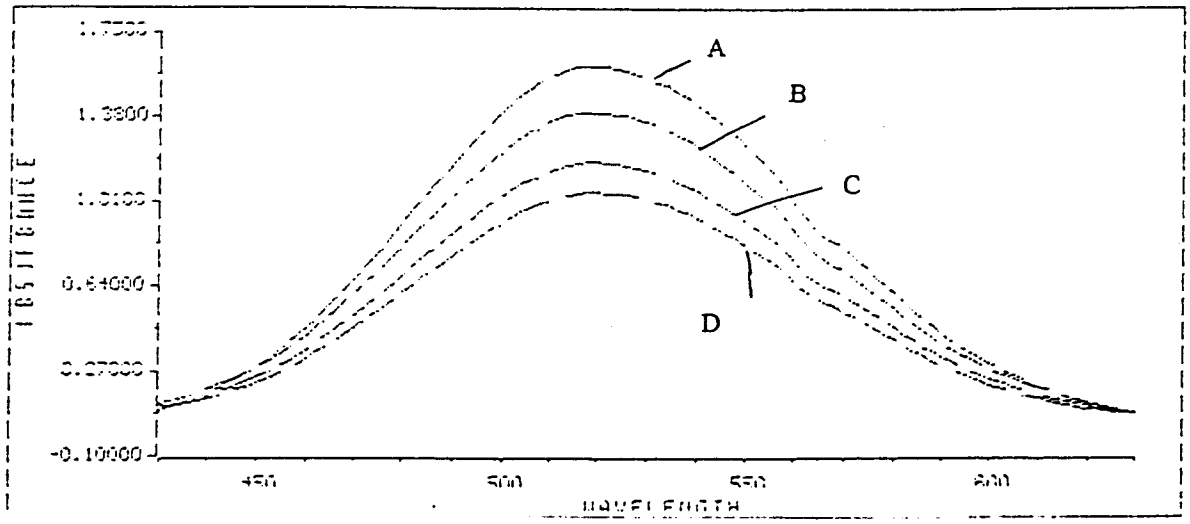

Figure 19 UV Spectra of GY(24) with Murexide
(A) GYC, (B) GY(24) at 0 min, (C) GY(24) at 5 min, and (D) GY(24) at 10 min.

ACETONITRILE MOBILE PHASE

Although acetonitrile would have been very easy to remove from the eluent of GY(24) fractions, no resolution of its early peaks occurred when this mobile phase was employed.

HEPTAFLUOROBUTYRIC ACID (HFBA)

The analytical concerns of this work involved good resolution and ease of purification following separation. Unfortunately, no protocol for removal of heptanesulfonate could be found.

One article suggested use of ion-pairing reagents in reversed-phase HPLC for successful isolation of peptides (*38*) . Early reagents were not volatile and could not be easily separated from the mixtures. For peptides of low polarity, the polar anion trifluoroacetic acid forms an ion-pair complex with the ammonium groups of the solute and its volatile nature permits easy removal from the eluent. Use of this reagent, however, may not permit sufficient retention on nonpolar columns of polar peptide mixtures to give adequate resolution. Other agents known as perfluoroalkanoic acids were shown to retain the peptide substantially longer than trifluoroacetic acid and can be removed by neutralization and freeze-drying followed by extraction with ether. Increased retention time is caused by the lipophilicity of the perfluoroalkyl groups, which effect a decrease in polarity of the resulting ion-pair. The longer the perfluoroalkanoic chain, the greater the retention factor. For this work, heptafluorobutyric acid (HFBA) was chosen and parameters such as injection size, flow rate and optimum temperature conditions were investigated.

Using 5 mM HFBA as mobile phase, excellent results occurred with injections of 50 μL of 5 mM Gly(std) monitored at 210 nm with a flow rate of 1.5 mL/min for 15.0 minutes. One peak at 3.466 minutes and two small negative system peaks were obtained.

An injection of GY(std) using identical conditions had two peaks, one at 3.298 min and another at 8.5 min. GY(24) had three major peaks at 1.933 min, 2.289 min and 3.246 min and several minor peaks (Figure 20).

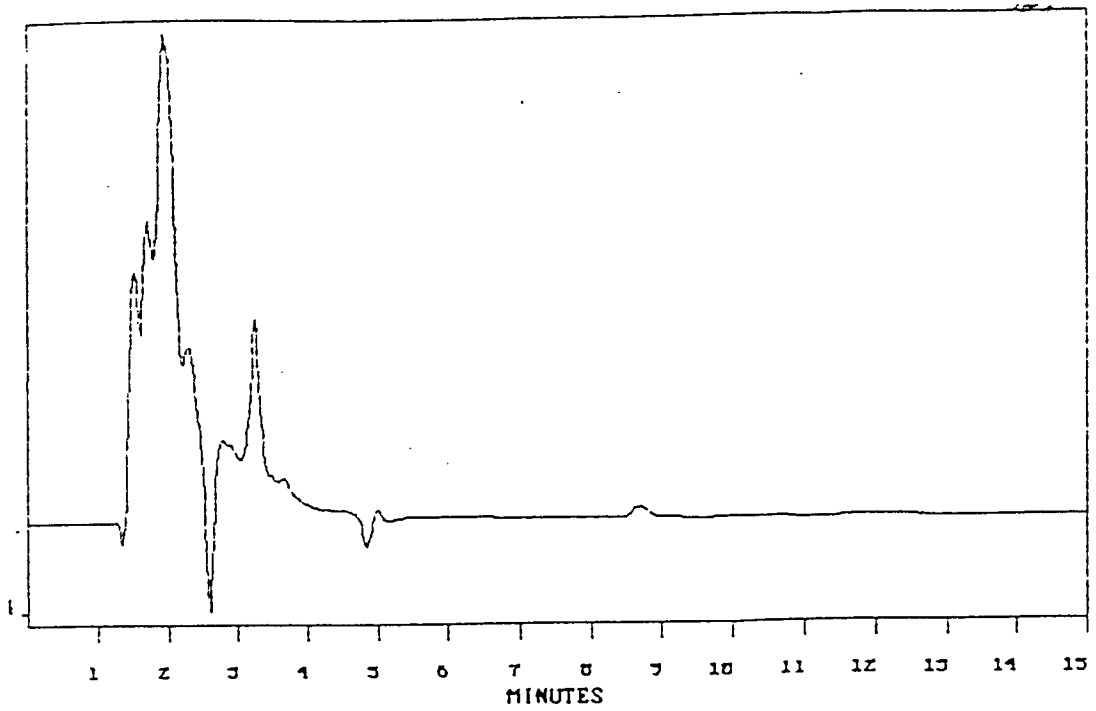

Figure 20 HPLC of 2.5 mM GY(24) (HFBA mobile phase, 30°C, flow rate of 1.5 mL/min, 210 nm)

Using 15:85(v/v) acetonitrile:HFBA as a mobile phase, Gly had multiple peaks for the first time, which deviated greatly from all other experiments to date. Further analysis with this mobile phase was abandoned.

Prior studies mentioned perfluoroalkanoic acids may not be completely transparent at 210 nm (*35*). Chromatograms were prepared using 5 mM HFBA in aqueous solution and monitored at 235 nm. A flow rate of 1.0 mL/min for 30 minutes revealed the

following peaks: 50 μL of 5 mM Gly had three peaks at 2.535, 5.285 and 7.113 min; 80 μL of 5 mM Gly had two peaks at 5.127 and 7.025 min; 100 μL of 5 mM Tyr had one peak at 7.072 min; 100 μL of 5 mM GY(std) had a major peak at 6.634 min and a minor peak at 15.958 min.

Results for GY(24) and HFBA run with 50 μL injections monitored at 235 nm for 30 minutes with a flow rate of 1.0 mL/min revealed four peaks: 2.405 min (6.9%), 3.018 min (31.8%), 3.723 min (10.8%), and 4.195 min (26.7%) (Figure 21). None of these appeared to match the Gly run at 235 nm.

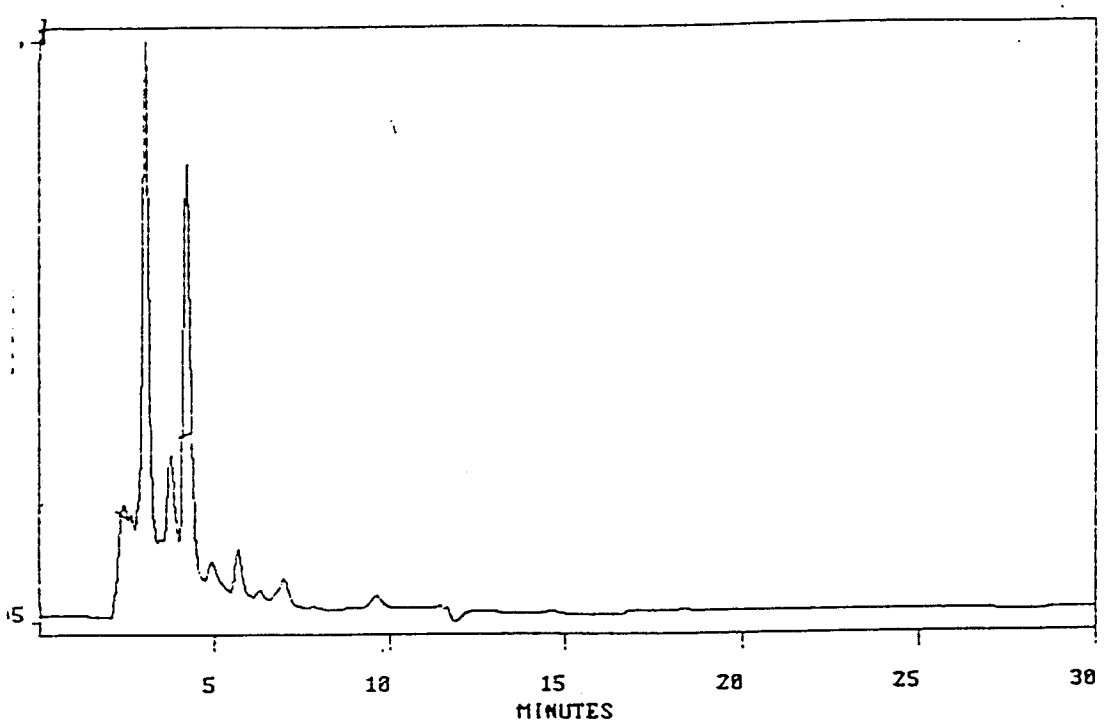

Figure 21 HPLC of 5 mM GY(24) (HFBA, 30°C, flow rate of 1.2 mL/min, 235 nm)

Using a variety of flow rates and 90 μL injections of GY(24) scanned at 210 nm, the following results occurred: 0.2 mL/min, six peaks were separated (11.595, 14.439, 17.953, 21.725, 23.695 and 27.068 min); 0.3 mL/min, a poor baseline was produced along with eight peaks (6.636, 7.317, 9.155, 10.279, 12.263, 13.924, 15.825 and 17.400 min); 0.4 mL/min, nine peaks were obtained (6.199, 7.324, 9.120, 11.558, 12.089, 13.793, 15.583, 17.058 and 23.80 min).

Chromatograms obtained using 50 μL samples with a flow rate of 0.5 mL/min monitored at 235 nm revealed the following: Gly had two peaks at 10.312 and 13.777 min; Tyr had two peaks at 9.608 and 13.847 min; GYC had two peaks at 4.412 and 13.689 min; and GY(24) had eight peaks at 4.732, 5.909, 7.324, 9.758, 11.101, 12.492, 13.675 and 19.068 min (Figure 22). Only one peak at 13.675 min corresponded to peaks for the Gly, Gly-Tyr or Tyr standards.

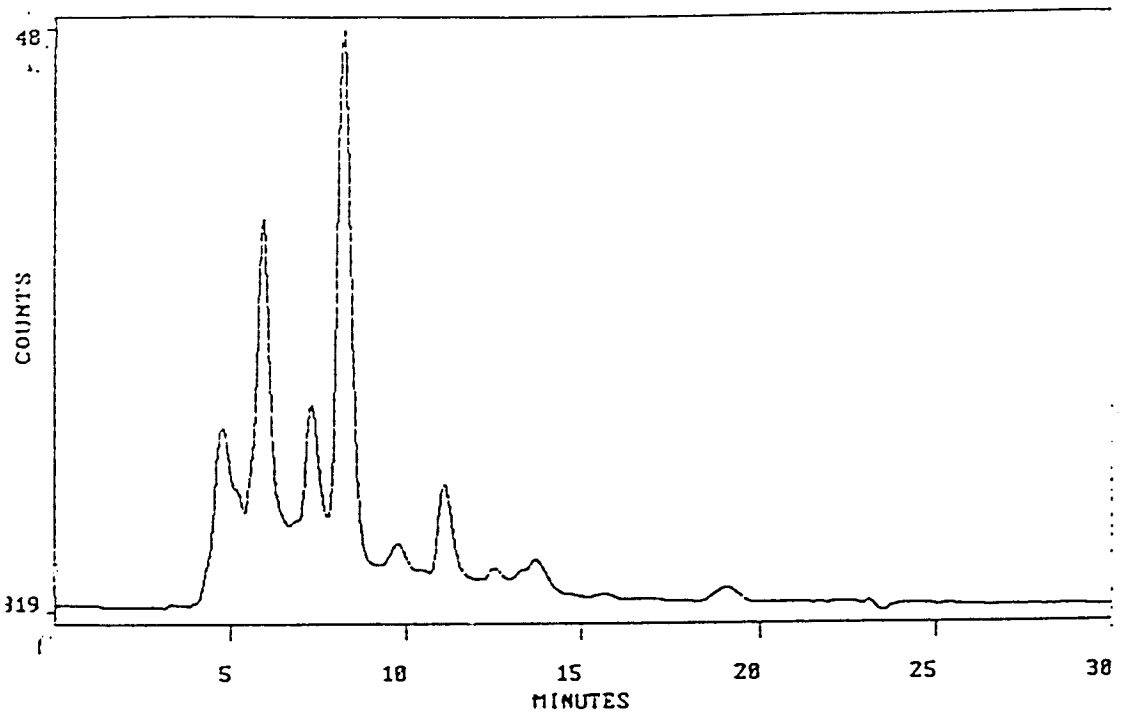

Figure 22 HPLC of 2.5 mM GY(24) (HFBA mobile phase, 30°C, flow rate of 0.5 mL/min, 235 nm)

HFBA WITH PERKIN-ELMER LIQUID CHROMATOGRAPH

Using the HPLC from the YSU Biology Department, the baseline problem and all the tremendous difficulties with programming a run were overcome. Very clean results for all samples were obtained as follows:

GYC at 210 nm and 235 nm had one peak at 12.82 min; Gly at 210 nm had two peaks, one at 9.84 and one at 12.55 min; Tyr at 210 nm had one peak at 12.73 min; and GY(24) at 210 nm had twelve peaks: 3.85, 4.61, 5.32, 6.78, 7.81, 9.27, 10.11, 12.60, 13.49, 17.17 and 19.35 min (Figure 23).

HPLC with catalase and mannitol controls revealed the following: Fe(III)/H_2O_2 had peaks at 3.85, 10.42 and 13.08 minutes; Fe(III)/H_2O_2/catalase at 3.85 and 12.55 minutes; Fe(III)/H_2O_2/catalase/mannitol at 3.85 and 12.55 minutes; GY(24)/catalase had fourteen peaks; GY(24)/catalase/mannitol had no peaks; and GY(24)/catalase/5-fold molar excess of mannitol had thirteen peaks.

Use of the IBM HPLC repeatedly produced two peaks for the Gly standard, which may have indicated a contaminated Gly sample. A new chromatogram with a fresh bottle of sample gave one peak at 9.53 minutes.

Working with timed GY samples exposed to the hydroxyl radical from 1-6 hours monitored at 210 nm with a flow rate of 0.5 mL/min, the following HPLC peaks were observed: GY(1) had one peak at 12.55 minutes (Figure 24); GY(2) had two peaks at 5.31 (minor) and 12.55 (major) minutes; GY(3) had two peaks at 5.31 (minor) and 12.59 (major) minutes; GY(4), GY(5) and GY(6) had two peaks at 5.37 (now major) and 12.60 minutes (Figure 25); GYC had one peak at 12.82 minutes; and Tyr had one peak at 12.73 minutes.

Late in the study, one more control, potassium phosphate buffer, was injected, monitored at 210 nm with a flow rate of 0.5 mL/min. Surprisingly, one major peak occurred at 12.43 minutes.

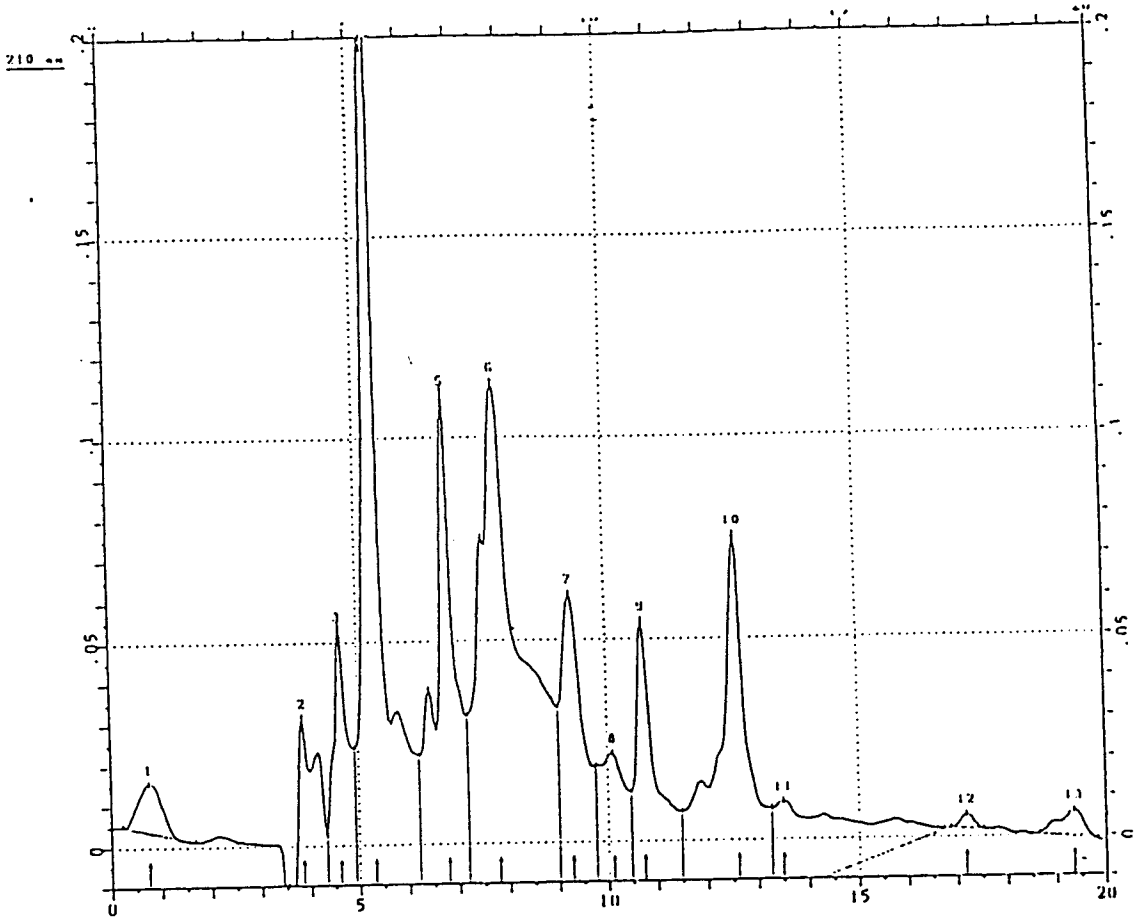

Figure 23 HPLC of 0.25 mM GY(24) (Perkin-Elmer LC, HFBA mobile phase, 210 nm, and flow rate of 0.5 mL/min)

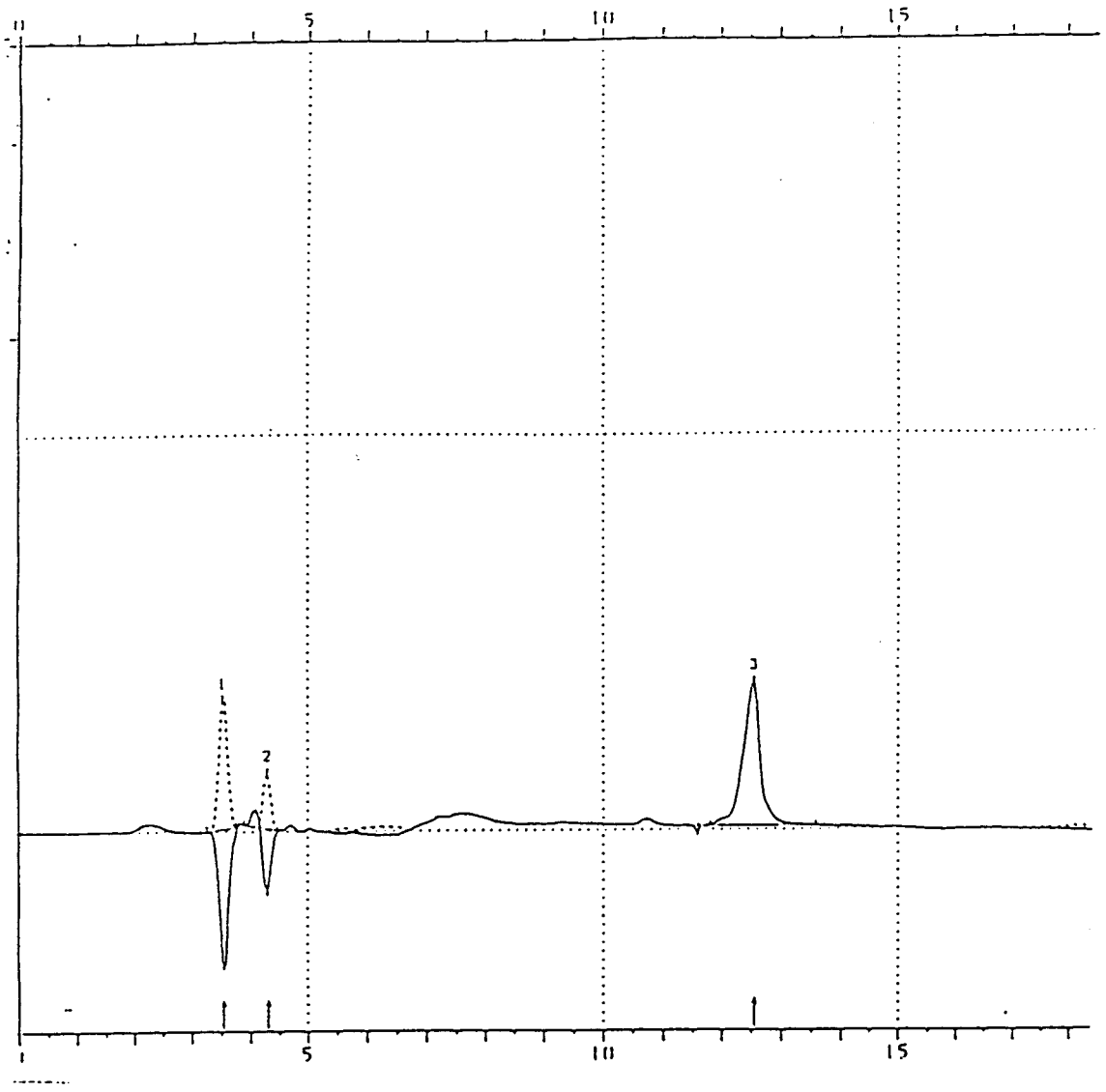

Figure 24 HPLC of GY after one hour exposure to free radicals (Perkin-Elmer LC, HFBA mobile phase, 210 nm, 0.5 mL/min)

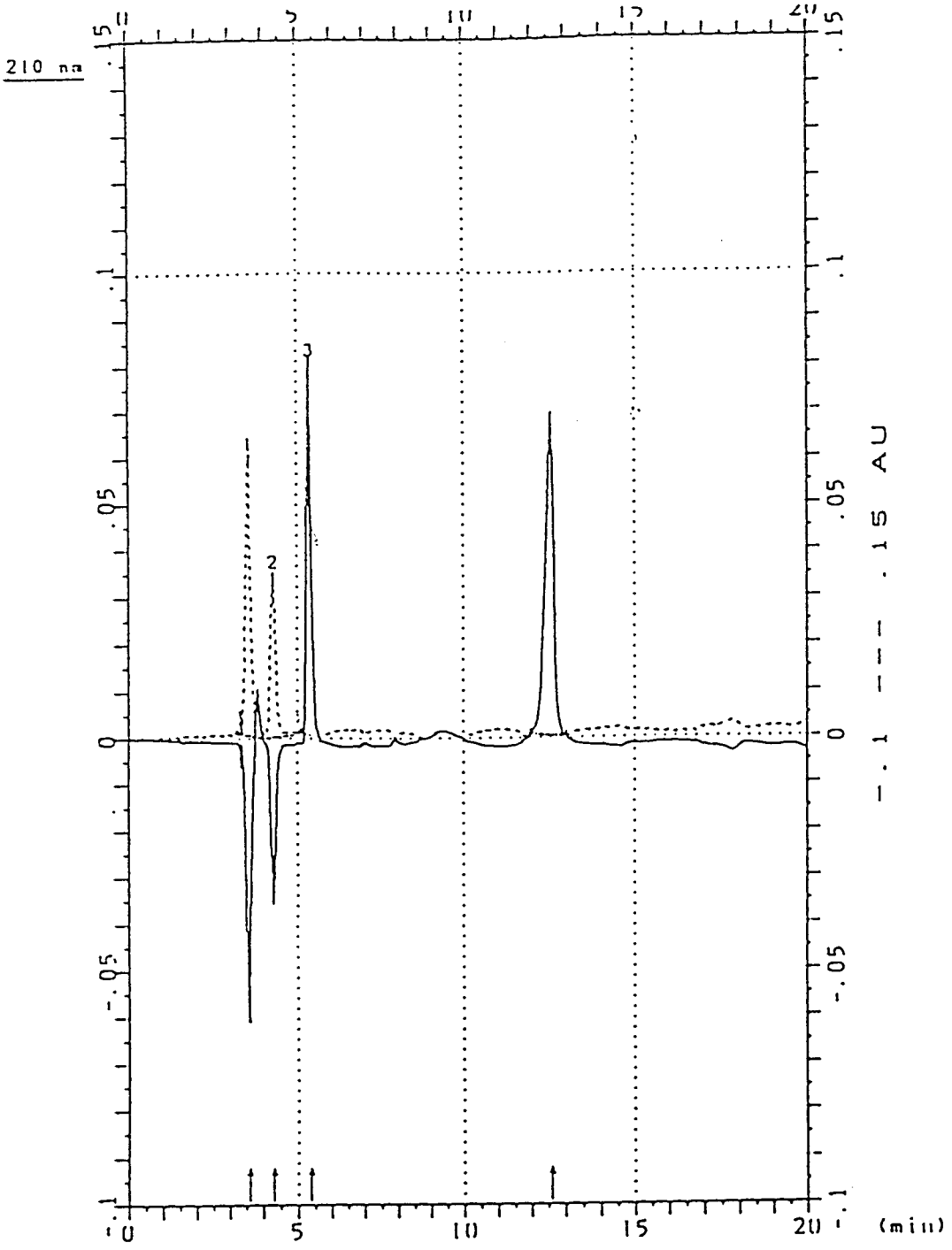

Figure 25 HPLC of GY after six hours exposure to free radicals (Perkin-Elmer LC, HFBA mobile phase, 210 nm, 0.5 mL/min)

Stage 4 Results: Separation of GY(24) through Other Chromatographic Techniques

OTHER SOLVENT SYSTEMS

Using aluminum backed silica gel TLC plates, a variety of mobile phases were used on GY(24) samples in an attempt to resolve the components present. Results of this TLC are presented in Table 12. R_f (1) values represented results using 70:30 (v/v) n-propanol:deionized water as the mobile phase; R_f (2) values used methanol as the mobile phase; and R_f (3) values used glacial acetic acid as the mobile phase. The use of n-propanol as a mobile phase produced of one spot with a R_f value of 0.491 for GY(24) which nicely corresponds to glycine (R_f of 0.492).

TABLE 12 TLC OF GY(24) WITH OTHER SOLVENT

Sample	*Rf (1)*	*Spot 1*	*Rf (2)*	*Spot 2*	*Rf (3)*	*Spot 3*
Gly	0.492	peach	0.133	pink	0.531	peach
GYC	0.669	gold	0.493	pale yellow	0.676	gold
GY(24)	0.491	peach	0.711	light spot	---	---

Ethyl acetate and dietyl ether were also used as TLC solvents; however, neither one showed any spots with Gly or GY(24). Using 2:2:1 (v/v) chloroform:methanol:17%NH_4OH for a TLC solvent produced one spot for Gly with a R_f of 0.69 and one for GY(24) with a R_f of 0.66, but no spot for the dipeptide.

PERCOLATION COLUMN CHROMATOGRAPHY

The upper layers of the first five fractions obtained from the freeze-dried GY(24) sample were yellow in color. Fifty-five fractions were collected over an 8-hour period. No color was seen with the remaining 50 fractions.

TLC of the 55 fractions using silica gel plates showed spots with only the first two fractions (Table 13):

Table 13 TLC of Fractions

Sample	*Rf*	*Spotting*
GYC	0.625	purple
Gly	0.431	purple
Tyr	0.805	purple
GY(24)	0.674	purple
Fraction 1	0.358, 0.247	purple
Top Fraction 1	0.491	purple
Bottom Fraction 1	0.45	purple
Top Fraction 2	0.412	purple
Bottom Fraction 2	---	---

Reversed-phase TLC results are listed in Table 14. The R_f value of the spot produced in the top layer of fraction 2 corresponds closely to glycine.

Table 14 Reversed-Phase TLC Fractions

Sample	*Rf*	*Spotting*
Gly	0.495	peach
GY(24)	---	---
Fraction 1	0.460, 0.400	peach
Fraction 2	0.491, 0.430	peach

DISCUSSION

The purpose of the research was to investigate whether cleavage of the peptide bond by hydroxyl radicals exhibits any site-specificity. Although a great deal of work has been examined on oxidative damage to proteins, little has been established about the site-specific nature of the fragmentation of the polypeptide chain due to reactive oxygen species. Specifically, the following issues were addressed: (1) can site-specific cleavage of the peptide bond be demonstrated? if so, (2) what parameters does cleavage depend on (e.g. temperature, pH, amino acid sequence)? and (3) does the use of different metal ions result in different patterns of fragmentation?

Evidence of Site-Specificity of Oxidation

Of all the dipeptides tested, preliminary results for Gly-Tyr and Gly-His exposed to free radicals for 24 hours showed the most promising results for further investigation. Experiments performed on seven dipeptides exposed to free radicals produced by iron (III) and hydrogen peroxide revealed evidence of fragmentation for only these two dipeptides. Significant differences in the UV spectra between 210-230 nm of the two dipeptides occurred after 24 hours incubation with hydroxyl radical. This may indicate a change in the peptide bond as peptide bonds absorb in this region. Both dipeptides produced a spot after TLC with a R_f value corresponding to glycine. Gly-His produced a number of other spots after TLC not corresponding to the other controls. Gly-Tyr had a second spot with a R_f value lower than the dipeptide or its standards when tested with Fe(III) and H_2O_2 using different solvent systems. Gly-Tyr exposed to Cu(II) and H_2O_2 produced two spots, again with a R_f value corresponding to glycine and one different than the dipeptide or tyrosine. Consistent changes in both the UV and TLC analysis of Gly-Tyr when exposed to free radicals lead to this dipeptide being the primary focus of the research.

Obtaining evidence of fragmentation for only two dipeptides leads to the suggestion that some site-specificity is involved. But why Gly-Tyr and Gly-His? In order for metal-catalyzed oxidation to be site-specific, the dipeptide must chelate a metal ion. To form a chelate ring with a metal ion bound at the α-amino nitrogen, the side chain of a free amino acid must contain a donor atom with an available electron pair (such as O, N or S). Multiple rings may form if the metal ion is also chelated by the α-amino and α-carboxylate groups (*43*). Glycine can chelate metal ion forming a five-membered, bidentate glycinate locus (Figure 26).

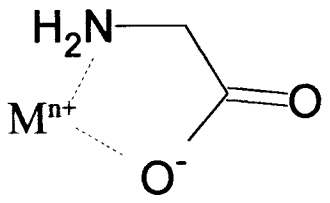

Figure 26 Glycinate Locus

The O atom on the side chains of Ser, Thr, Asp, Asn, Glu and Gln, the S atom on the side chains of Cys and Met, and the N atoms on the side chains of Asn, His, Arg and Lys are examples of donor atoms available for potential chelation. Tyr and Pro are sterically inhibited from forming a chelate with their hydroxyl groups and their glycinate loci. His likely chelates a metal ion to its amino nitrogen and the pyridine nitrogen of its imidazole ring. The literature suggests weak interactions between the aromatic side chains of Phe, Tyr and Trp with Cu(II) (*43*).

A coordination complex of Cu(II) with some simple dipeptides was found to occur between the amino nitrogen, the deprotonated peptide amide nitrogen and the carboxylate oxygen (Figure 27)(*44*).

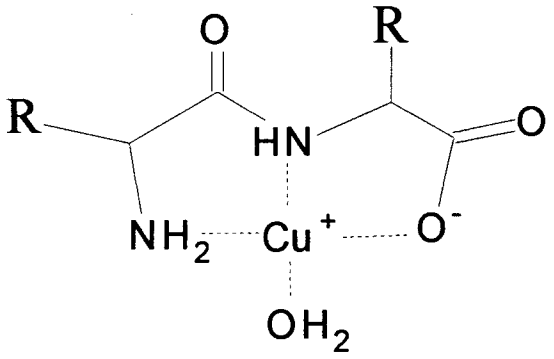

Figure 27 Coordination Complex of Dipeptide

Such information suggests all the dipeptides tested should be able to coordinate the metal ion between the α-amino and the carboxyl terminus. Yet only Gly-Tyr and Gly-His resulted in modification. Although the amino acid tyrosine is unlikely to form a metal coordinate with its glycinate locus and large phenolic hydroxyl group, perhaps a chelate is formed with the dipeptide Gly-Tyr. The free rotation of glycine may bring it within van der Waals distance of the aromatic ring of tyrosine. Observations from X-ray crystallography revealed a weak interaction between the empty "d" orbital of Cu(II) and the six-π electron system of tyrosine's aromatic ring with a bond distance of 3.17 - 3.32 Angstroms (*45*). The fact that Pro-Tyr was not modified significantly may support this hypothesis, as the bulkier side chain of proline may exceed the preferred distance for interaction. The most stable configuration for Gly-Tyr is one in which the carboxyl group is trans to the aromatic ring. NMR studies of Pd(II) complexes of Gly-Tyr show ligand bound through the carboxyl group, the α-amino nitrogen, and the deprotonated nitrogen of the peptide bond at pH 3-12. In addition, possible interaction between the aromatic ring and the Pd(II) through axial "d" orbitals has been suggested, producing a rigid structure for the chelate ring (*46*). Perhaps the aromatic ring of tyrosine lies in a plane above the metal ion complex illustrated in Figure 27, forming a stable dipeptide-metal ion

complex. Formation of the hydroxyl radical by interaction between metal ion and H_2O_2 could then lead to peptide bond cleavage possibly by the α-amidation process.

Timed reactions, ammonia assay tests, acetylation-deacetylation experiments, derivatization of the N-terminus, use of the free radical scavenger mannitol, and variations in hydrogen peroxide and Fe(III) concentrations with Gly-Tyr were investigated.

The ammonia assay of Gly-Tyr indicated the production of ammonia, which suggests deamination, but no linear relationship was found over time. The disappearance of the dipeptide spot with TLC analysis supports this possibility.

There was no modification of the dipeptide in the presence of mannitol, which suggests either damage was not site-specific or perhaps mannitol chelates the metal and prevented reaction. Further testing with thiourea would be helpful in analyzing these results.

Acetylation of Gly-Tyr was pursued to investigate how alteration of tyrosine affects metal-catalyzed oxidation. Should chelation with metal ion involve interactions with the phenolic hydroxyl of tyrosine, modification of this site may affect the oxidative reaction occurring. Experiments attempting to acetylate Gly-Tyr at the phenolic hydroxyl group encountered several difficulties: (1) water in the solution causes extensive hydrolysis of the anhydride, requiring high concentrations of acetic anhydride to acetylate Gly-Tyr; and (2) high concentrations of acetic anhydride (above 0.08 M) may have also acetylated the α-amino group of glycine. In order to verify that only acetylation of the phenolic hydroxyl group had occurred, use of hydroxylamine was suggested (*40*). It is successful at deacetylating only the phenolic hydroxyl group. Unfortunately, when the presumably acetylated Gly-Tyr was treated with hydroxylamine, there was no indication of a spot corresponding to the dipeptide control. Use of tetrahydrofuran as a solvent may enable use of less acetic anhydride, as it will not hydrolyze the acetic anhydride, permitting lower concentrations which would prevent the acetylation of the α-amino group. A search of the literature proposed the simultaneous use of perchloric acid with acetic

anhydride to produce O-acylation. The presence of perchloric acid blocked the acetylation of the amino group (*41*). Future work in this area may incorporate this suggestion to obtain the desired product.

Interested in acetylating the phenolic hydroxyl group of Gly-Tyr without acetylation of the N-terminus, another project involving an attempt to mask the α-amino group of Gly-Tyr using carbobenzoxy chloride was pursued. The modified Gly-Tyr should have a protected N-terminus and upon exposure to acetic anhydride, only acetylation of the phenolic hydroxyl group should occur. Removal of the CBZ would have been followed by exposure of the acetylated Gly-Tyr to free radicals. Ultimately, the goal was to investigate the effects of modification of the Gly-Tyr on the free radical reaction observed. The reaction between carbobenzoxy chloride and glycyltyrosine produces carbobenzoxyglycyltyrosine, which contains an amide bond (eq. 22) .

$$C_6H_5CH_2OCOCl + H_2NCH_2CONHCH(CH_2C_6H_5OH)COOH \longrightarrow C_6H_5CH_2OCONHCH_2CONHCH(CH_2C_6H_5OH)COOH \quad (22)$$

TLC visualized with ninhydrin revealed a spot different than the dipeptide control, indicating the procedure did not mask the α-amino function since ninhydrin reacts with only primary and secondary amines. However, a spot with Pauly Reagent suggests the procedure was successful. Attempts to isolate and crystallize the CBZ-Gly-Tyr did not work, preventing further analysis of this product.

Parameters for Oxidative Reactions

When the concentration of Fe(III) and H_2O_2 were reduced below 150 μL, the R_f values of spots on TLC plates were close to the control, which indicated a minimum of 150 μL of Fe(III) and 150 μL H_2O_2 were needed for complete reaction.

Copper (II), iron (II) and cobalt (II) appear to cause metal-catalyzed modification of the dipeptides tested and would warrant further investigation. Results with Cu(II) and Co(II) suggest a different process than with Fe(II). Both Cu(II) and Co(II) had TLC spots corresponding to their respective N-termini, but Fe(II) had no spots corresponding to the dipeptide or amino acid controls. Fe(II) results may indicate deamination occurred. TLC of the Ni(II) sample revealed some modification occurred, although the spot did not correspond to the dipeptide or the amino acid controls.

Separation of Reaction Products

Reversed-phase columns of alkylsilane-bonded silica retain peptides through hydrophobic interactions (*35*). HPLC separations of amino acids are complicated by their wide range of polarities, making isocratic analysis very difficult. In addition, most have low UV extinction coefficients and require the use of very pure solvents. Very polar amino acids require an ionic surfactant in the mobile phase to increase their retention. For clear resolution and sharp peaks, phosphate buffers have been used to form hydrophilic ion pairs with protonated amino groups. However, the phosphate buffer is not volatile, making post-column purification difficult. Acetic acid gives longer retention times, but very broad peaks (*35*). Trifluoroacetic acid is volatile, but polar peptides are not retained long enough with its use for resolution. The literature (*42*) describes use of copper(II) and alkylsulfonate as ion-pair reagents in the mobile phase as viable alternatives. Cu(II) ions are known to form charge-transfer complexes with amino acids, increasing their retention time. Maximum absorption occurs at 235 nm. Polar solutes still move very quickly through the column, requiring the addition of a hydrophobic ion-pairing reagent such as the alkylsulfonates (*42*). The retention of the solutes increases with increasing length of alkyl sulfonate chain and with increasing concentration. Complexation with Cu(II) is more favorable at high pH, but above 6 will precipitate out as $Cu(OH)_2$. Thus a buffer in the mobile phase is required to prevent precipitation. Acetate, buffered at pH 5.6

was selected in trial studies. Thorough rinsing of the column with EDTA was used daily to prevent Cu(II) attack on the metal parts of the column and its uptake by the stationary phase silanols. The alkylsulfonate is absorbed on the reversed phase via hydrophobic interactions. The presence of the negative sulfonates will retard the Cu(II) ion complexes on the column. In an attempt to determine the best resolution of the reaction products, factors such as temperature, flow rate, injection volumes and concentration of alkylsulfonate were investigated.

Initial attempts to analyze the reaction products of GY(24) using 5 mM heptanesulfonate with 0.5 mM Cu(II) as the mobile phase quickly indicated the need to use injection volumes no greater than 40 μL. Larger injections overloaded the system as indicated by broad peaks. Flow rates could not exceed 2.0 mL/min; otherwise, excessive pressures caused leaks. Initial concentrations of 5 mM standards also produced very broad peaks; dilutions to 0.5 mM alleviated this problems. Operating the HPLC at 30 °C, with 40 μL injections of 0.5 mM concentrations of standards and a flow rate of 1.2 mL/min produced peaks for the dipeptide and amino acid controls within a 30 minute run.

Attempts to identify the standard peaks by collecting eluent and subjecting it to TLC and UV analysis were unsuccessful. The solutions were too dilute for detection and larger injections or higher concentrations could not be used with the HPLC.

The negative peaks associated with the Cu(II)/heptanesulfonate mobile phase were effectively diminished by diluting 5 mM standards to 0.5 mM with the mobile phase. Although tyrosine had revealed a peak in earlier trials, it disappeared completely with the samples diluted with mobile phase. Increasing the temperature to 40 °C and increasing the run time to 75 minutes eventually resulted in the elution of tyrosine. A drawback of operating at higher temperatures was the resulting instability of the baseline. Reducing the concentration of the heptanesulfonate was another way to reduce the retention time of tyrosine. Use of 0.8 mM heptanesulfonate buffer operating at 40 °C with 40 μL injections of 0.5 mM standards, diluted with mobile phase as described above, provided peaks for all

dipeptide and amino acid controls within a 30 minute run, as well as strong, although crowded peaks for GY(24).

Once the parameters for obtaining peaks for all samples were determined, focus turned to resolution of GY(24) peaks. Optimum separation occurred with 2.5 mM heptanesulfonate operating at 40 °C with a flow rate of 1.2 mL/min and an injection volume of 60 μL of 2.5 mM GY(24).

Although conditions for optimum resolution of peaks were found using heptanesulfonate as mobile phase, its removal from eluent for further sample analysis, particularly NMR, was a problem. Further investigations pursued the use of heptafluorobutyric acid (HFBA) as the ion-pairing reagent, which can be removed for product analysis.

Chromatograms prepared on the IBM/LC HPLC using 5 mM HFBA, scanned at 235 nm with a flow rate of 0.5 mL/min and 50 μL injections produced the best separation of GY(24). Eight peaks were revealed. Continuous baseline problems as well as very long equilibration times greatly hampered research efforts. Further investigation using the Perkin-Elmer Liquid Chromatograph was pursued.

All standards and dipeptide controls using the 5 mM HFBA mobile phase produced consistent results. Multiple peaks for some of the standards disappeared. Chromatograms of GY(24) continued to show increased resolution, with twelve peaks in all. An analysis of the chromatogram of Fe(III)/H_2O_2/catalase at the same concentrations found in the trials matched two of the twelve peaks. Timed studies of Gly-Tyr revealed a peak at 12.55 minutes in the first hour of exposure to Fe(III) and H_2O_2. From two to six hours of exposure, the 12.55 minute peak became smaller while a new peak at 5.37 minutes appeared and increased.

Although phosphate salts with low absorption in the UV at 215 nm are acceptable for use in reversed-phase HPLC, a test run of the KPi buffer used in all sample dilutions produced a chromatogram with one major peak at 12.43 minutes. This certainly explains

the second, unidentifiable peak obtained with all the standards. It also explains the lack of UV absorbance which occurred with eluent collected on the 12 minute peak of the GY(std).

CONCLUSION AND FURTHER DIRECTIONS

In essence, a survey was conducted to investigate the site-specificity of the hydroxyl radical. Did cleavage take place? Admittedly, results were ambiguous but they were suggestive. Gly-Tyr and Gly-His consistently displayed signs of alteration, while other model dipeptides did not. The consistent appearance of spots with R_f values corresponding to the N-terminus of the dipeptide suggest that fragmentation occurred.

One of the most interesting aspects of this project was the resolution of peaks of the GY(24) sample by HPLC. Something is definitely occurring. An attempt to collect the eluent corresponding to the different peaks would be an important step for future studies. Heptafluorobutyric acid produced the most consistent separations of reaction products. Continued use of this mobile phase is recommended. Eluent samples should be tested for possible identification by TLC and reintroduction into HPLC. Purification of eluent samples should be pursued, as the heptafluorobutyric acid can be removed as previously discussed. In addition, monitoring the reaction products between the six and twenty-four hours used in this research should help pinpoint the changes in the modified Gly-Tyr over time.

An investigation into the nature of the precipitate formed in the reaction of Gly-Tyr with free radicals may provide further insight into the identity of possible reaction

products. Different solvent systems should be investigated for ultimate solubilization of this product, followed by TLC, HPLC, NMR and mass spectrometry studies.

Model tripeptides (e.g. GGY) might be used to investigate the metal chelation proposed in this research between the glycinate locus and the aromatic ring of tyrosine. Other modifications of the dipeptide (e.g. acetylation of the phenolic hydroxyl and carboxyl groups) may shed light on the nature of the metal ion complex described earlier. Will loss of this site prevent the complex from forming and how will this affect the reaction with free radicals?

There are many directions in which this project could be pursued in depth. This research generated as many questions as it answered. Each aspect investigated is worthy of consideration as a separate research project. The evidence presented throughout seems to confirm there is something unique about the nature of dipeptides such as Gly-Tyr and Gly-His, causing them to react differently with free radicals than other dipeptides. A pursuit of the identification and isolation of their reaction products would be the next major project to further investigate the site-specificity of the hydroxyl radical.

REFERENCES

1. Halliwell, B. (1987) *FASEB J.* **1**, 358-364.
2. Stadtman, E.R. (1990) *Free Radical. Biol. Med.* **9**, 315-325
3. Halliwell, B. and Gutteridge, J. (1984) *Biochem. J.* **219**, 1-14.
4. Halliwell, B. and Cross, C.E. (1994) *Environ. Health Perspect. Suppl.* **6** *(10)*, 5-12.
5. Stadtman, E. and Berlett, B. (1997) *Chem. Res. Toxicol.* **10**, 485-494.
6. Halliwell, B. and Gutteridge, J.M.C. (1985) *Molec. Aspects Med.* **8**, 89-193.
7. Okada, Shigeru (1996) *Pathology International* **46**, 311-332.
8. Winter, M.L. and Liehr, J.G. (1991) *J. Biol Chem.* **266**, 14446-14450.
9. Sohal, R.S., Agarwal, S., Dubey, A. and Orr, W.C. (1993) *Proc. Natl. Acad. Sci. U.S.A.* **90**, 7255-7259.
10. Oliver, C.N., Starke-Reed, P.E. et. al. (1990) *Proc. Natl. Acad. Sci. U.S.A.* **87**, 5144-5147.
11. Cross, C.E., Reznick, A.Z. et al. (1992) *Free Radical Res. Commun.* **15**, 347-352.
12. Reznick, A.Z., Cross, C.E. et al. (1992) *Biochem. J.* **286**, 607-611.
13. Sohal, R.S., Ku, H.-H. and Agarwal, S. (1993) *Biochem. Biophys. Res. Commun.* **196**, 7-11.
14. Wieland, P. and Lauterburg. B.H. (1995) *Biochem. Biophys. Res. Commun.* **213**, 815-819.
15. Oliver, C.N., Ahn, B.-W. et. al. (1987) *J. Biol Chem.* **262**, 5488-5491.
16. Stadtman, E.R. and Oliver, O.N. (1991) *J. Biol. Chem.* **266** (*4*), 2005-2008.
17. Neuzil, J., Gebiki, J.M. and Stocker, R. (1993) *Biochem. J.* **293**, 601-606.
18. Farber, J.M. and Levine, R.L. (1986) *J. Biol. Chem.* **261**, 4574-4578.

19. Sahakian, J.A., Shames, B.D. and Levine, R.L. (1991) *FASEB J.* **5**, A1177 (Abstract).

20. Friguet, B., Szweda, L. and Stadtman, E.R. (1994) *Arch. Biochem. Biophys.* **311**, 168-173.

21. Chevion, M. (1988) *Free Radical. Biol. Med.* **5**, 27-37.

22. Deasey, C., Broerman, M., Shively, S., Alexander, A., & Hart, V. (1970) *J. Amer. Leather Chem. Assoc.* **65**, 537-546.

23. Creeth, J.M., Cooper, B., Donald, A.S.R., & Clamp, J.R. (1982) *IRCS Med. Sci.: Libr. Compend.* **10**, 548-549.

24. Carmichael, P.L., Hipkiss, A.R. (1991) *Free Rad. Res. Comms.* **15***(2)*, 101-110.

25. Ookawara, T., Kawamura, N., Kitagawa, Y., Taniguchi, N. (1992) *J. Biol. Chem.* **267** *(26)*, 18505-18510.

26. Garrison, W.M. (1987) *Chem. Rev.* **87**, 381-398.

27. Swallow, A.J. (1960) *In Radiation Chemistry of Organic Compounds.* (Swallow, A.J. Ed.): Pergamon Press, New York, 211-224.

28. Schuessler, H. and Schilling, K. (1984) *Int. J. Radiat. Biol.* **45**, 267-281.

29. Stadtman, E.R. and Berlett, B.S. (1991) *J. Biol. Chem.* **266(26)**, 17201-17211.

30. Stadtman, E.R. (1993) *Annual Review of Biochemistry* **62**, 797-821.

31. Huggins, T.G. et. al. (1993) *J. Biol. Chem.* **268**, 12341-12347.

32. Nadkarni, D.V. and Sayre, L.M. (1995) *Chem. Res. Toxicol.* **8**, 284-291.

33. Mullarkey, C.J., Edelstein, D. and Brownlee, M. (1990) *Biochem. Biophys. Res. Commun.* **173**, 932-939.

34. Friguet, B., Stadtman, E.R. and Szweda, L. (1994) *J. Biol. Chem.* **269**, 21639-21643.

35. Hancock, W.S. & Harding, D.R.K. "Review of Separation Conditions," in *CRC Handbook of HPLC for the Separation of Amino Acids, Peptides, and Proteins, Volume I.*

36. Voet, D. & Voet, J.G. (1990) *Biochemistry.* Wiley: New York, Chapters 4-6.

37. Hancock, W.S. and Harding, D.R.K. "Review of Separation Conditions," in *CRC*

Handbook of HPLC for the Separation of Amino Acids, Peptides, and Proteins, Volume II.

38. Harding, D.R.K., Bishop, C.A., et. al. (1981) *Int. J. Peptide Protein Res.* **18**, 214-220.

39. Shaltiel, S. and Patchornik, A. (1963) *J. Amer. Chem. Soc.* **85**, 2799-2806.

40. Ohnishi, M., Suganuma, T. and Hiromi, K. (1974) *J. Biochem.* **76**, 7-13.

41. Greenstein, J.P. and Winitz, M. (1961) *Chemistry of the Amino Acids, Vol. II,* John Wiley and Sons, Inc., 891-895.

42. Levin, Shulamit and Grushka, Eli. (1985) *Anal. Chem.* **57**, 1830-1835.

43. Sigel, Helmut. (1979) *Metal Ions in Biological Systems, Vo. 9.* Marcel Dekker,Inc., NY.

44. Farkas, E. and Kiss, T. (1989) *Polyhedron* **8** (20), 2463-2467.

45. Franks, W.A. and Van der Helm, D. (1970) *Acta Crystallogr.* **B27**, 1299.

46. Kozlowski, Henryk and Jezowska, Malgorzata (1977) *Chemical Physics Letters* **47**(3), 452-456.